2-17-2012 12:00 AM

Targeted Intracellular Therapeutic Delivery Using Liposomes Formulated with Multifunctional FAST proteins

Rae L. Nesbitt
The University of Western Ontario

Supervisor
Dr. John Lewis
The University of Western Ontario

Graduate Program in Medical Biophysics
A thesis submitted in partial fulfillment of the requirements for the degree in Master of Science

TARGETED INTRACELLULAR THERAPEUTIC DELIVERY USING LIPOSOMES FORMULATED WITH MULTIFUNCTIONAL FAST PROTEINS

(Spine Title: Targeted Therapy using Fusogenic Liposomes)

(Thesis format: Monograph Article)

by

Rae-Lynn Nesbitt

Graduate Program in Medical Biophysics: Molecular Imaging

A thesis submitted in partial fulfillment
of the requirements for the degree of
Master of Science

The School of Graduate and Postdoctoral Studies
The University of Western Ontario
London, Ontario, Canada

THE UNIVERSITY OF WESTERN ONTARIO
School of Graduate and Postdoctoral Studies

CERTIFICATE OF EXAMINATION

Supervisor

Dr. John Lewis

Supervisory Committee

Dr. Joe Mymryk

Dr. Jeff Carson

Examiners

Dr. Savita Dhanvantari

Dr. Alison Allan

Dr. Dwayne Jackson

The thesis by

Rae-Lynn Nesbitt

entitled:

Targeted Intracellular Therapeutics Using Liposomes Formulated with Multifunctional FAST Proteins

is accepted in partial fulfillment of the
requirements for the degree of
Master of Science

Date

Chair of the Thesis Examination Board

Abstract

Prostate cancer is the most common malignancy in North American men and there is no treatment currently available which offers a clear survival advantage to patients with prostate cancer. We studied liposomes formulated with the fusion-associated small transmembrane (FAST) protein, p14. In this study, we hypothesized that therapeutics delivered in molecular targeted fusogenic liposomes will increase intracellular delivery and specificity for prostate cancer. We demonstrated that liposomes formulated with p14-bombesin significantly increased the delivery of fluorescein isothiocyanate (FITC) into human prostate cancer (PC-3) cells compared to either standard liposomes or non-targeted fusogenic liposomes. Delivery of FITC to benign prostate hyperplasia (BPH) cells, which express low levels of the gastrin releasing peptide receptor (GRPR), was similar for targeted and non-targeted formulations. Specificity for GRPR was further established by knocking down GRPR expression with siRNA. Knockdown of the receptor resulted in equivalent intracellular delivery of the FITC with targeted and non-targeted formulations.

Keywords: Bombesin, Fusogenic Liposomes, p14, Prostate Cancer, Targeted Therapy

Acknowledgements

I would like to begin my acknowledgments with my supervisor Dr. John Lewis. Lewis is a great mentor whose valuable research experience influenced the researcher I have become. I have enjoyed the time spent pursuing a research dream in his laboratory. I have gained valuable experience and confidence as young trainee.

I would like to thank the integral person responsible for my research career, Dr. Gabriel Chan. Gabe entrusted me with his transplant project to execute experiments and organize my time as inexperienced undergraduate student. I owe my research abilities to his wife Dr. Brigitte Goulet who dedicated her free time as a busy cancer researcher to teach me the techniques necessary to become a successful trainee. I would also like to thank Amber Ablack, who also spent her time training in tissue culture.

Furthermore, I would like to thank my advisory committee, Dr. Joe Mymryk and Dr. Jeff Carson who were instrumental in my progress by providing critical insight during meetings.

I will forever be grateful to all the members of the Lewis laboratory, for their guidance, support and laughs. The Lewis lab was an exciting and comforting environment to work in and I would like to express my gratitude to Amber Ablack, Amy Robertson, Balaji Iyengar, Bhavik Monocha, Catalina Vasquez, Chen Lu, Hon Leong, Fong Cho, Laura Fung and, Navid Baktash. Special thanks to Dr. Desmond Pink for the support and encouragement through this exciting journey.

I am extremely fortunate for my exceptional family and I thank my mom, dad, and sister who have also been instrumental in encouraging my career path. Their overwhelming support and encouragement not only in this journey but throughout my entire life, has created the

determined and goal driven person I am today. You believed in me in times I lost sight of my capabilities and your perseverance pushed me to see a superior self.

Above all, I would like to thank Phil for supporting me through the rough days until I found success. Thank you for your tolerance and love. I could not have done this without you. This experience has reaffirmed what love and companionship means, stand by one another through thick and thin.

Dedication

I dedicate this to my family, friends, and Phil whom always saw the light at the tunnel when I sought darkness. Thank you.

I may not be there yet, but I'm closer than I was yesterday.

~Author Unknown

Table of Contents

List of Tables

List of Figures

Appendix

List of Abbreviations

ANOVA: Analysis of variance

ARV: Avian Orthoreovirus

BBV: Baboon Orthoreovirus

BPH: Benign Hyperplasia Prostate Cells

Chol: Cholesterol

CPP: Cell Penetrating Peptide

DC-Chol: dimethylaminoethane-darbamoyl-cholesterol

DLS: Dynamic Light Scattering

DMEM: Dulbecco's Modified Eagle Medium

DNA: deoxyribonucleic acid

DOPC: 2-dioleoyl-sn-glycerol-3 phosphatidylcholine

DOPE: 1, 2-dioleoyl-sn-glycerol-3 phosphatidylethanolamine

DOTAP: 1, 2-dioleoyl-3-trimethylammonium-propane

DOTMA: 1-2, 3-dioleyloxy-propyl-trimethylammonium chloride

EPR: Enhance Permeability and Retention

EtBr: Ethidium Bromide

FAST: Fusogenic Associated Small Transmembrane

FBS: Fetal Bovine Serum

FITC: Fluorescein isothiocyanate

FRET: Fluorescence Resonance Energy Transfer

G protein: Glycoprotein

GRP: Gastrin Releasing Peptide

GRPR: Gastrin Releasing Peptide Receptor

HP: Hydrophobic Patch

LfcinB: Bovine lactoferricin

mAb: monoclonal Antibody

MOI: Multiplicity of Infection

MRV: Mammalian Orthoreovirus

MWM: Molecular Weight Marker

NBV: Nelson Bay Reovirus

OD: Optical Density

OG: n-Octyl b-D-glucopyranoside

pAb: Polyclonal Primary Antibody

PBS: Phosphate Buffered Solution

PC3: Prostate Cancer Cells

PCa: Prostate Cancer

PCR: Polymerase Chain Reaction

PEG: Polyethylene Glycol

PSA: Prostate Specific Antigen

PVDF: Polyvinylidene difluoride

RPM: Revolution Per Minute

RRV: Reptilian Reovirus

QM5: Quail Fibrosarcoma Muscle Cells

SDS-PAGE: Sodium Dodecyl Sulfate-Polyacrylamide Gel Electrophoresis

SEM: Standard error of the mean

Sf21: *Spodoptera frugiperda* insect cells

siRNA: small interfering ribonucleic acid

SP HP: Sepharose High Performance column

Std: Standard

TBE: Tris/Borate/EDTA buffer

TBST: Tri-Buffered Saline and Tween 20

VSV: Vesicular Stomatitis Virus

WS: Wrapsomes

Chapter 1

1 Introduction

1.1 Overview of Prostate Cancer

Epidemiology

Cancer is a global epidemic and a major health burden with approximately 180,000 new cases in Canada alone this year (Canadian Cancer Statistics, 2011). An estimated 75,000 Canadians succumbed to this disease in 2011 (Andriole et al., 2009; Canadian Cancer Statistics, 2011). The term cancer in lay is a variety of diseases characterized by out of control cell growth. Prostate cancer is the most common cancer in Canadian men with a lifetime risk of 1 in 7 and a mortality rate of 1 in 27 (Canadian Cancer Statistics, 2011). Prostate cancer is predominately diagnosed between men of 60-69 years of age and if diagnosed at an early stage, 98% of cases are curable (Andriole et al., 2009; Canadian Cancer Statistics, 2011; Gomella et al., 2011; Jacobsen et al., 1995). Although prostate cancer has been hailed to be a "slow growing cancer", the incidence rate has increased more rapidly in past years (Canadian Cancer Statistics, 2011; Gomella et al., 2011). This increase in diagnosis may be due to the aging population, the evolution of medical technology and the routine blood screen for prostate specific antigen (PSA) (Ellison, Gibbons, & Canadian Cancer Survival Analysis Group, 2001; Gomella et al., 2011; Jacobsen et al., 1995). Conversely, prostate cancer is also the most common malignancy in North American men, accounting for 10% of all cancer-related deaths in 2010 (Andriole et al., 2009; Ellison et al., 2001).

Origin

A cancer of the glandular epithelium, prostate cancer is classified as an adenocarcinoma. Prostate cancer risk is determined largely by age however, other risk factors are genetic predisposition, dietary habits, and environmental stressors. Although prostate cancer is the most common malignancy in males, the cell of origin in the gland remains unclear. Prostate cancer has been thought to arise from cell expansion of luminal cells and the absence of basal cells in the epithelium of the prostate gland (Lawson et al., 2010). However, recently researchers have identified that basal cells can also initiate prostate cancer (Goldstein et al., 2010) and therefore both the basal and luminal cells have now been identified as prostate cancer cells of origin (Lawson et al., 2010). Even though prostate cancer is a slow growing cancer it still maintains the ability to metastasize. Once prostate cancer spreads, the cancer predominantly metastasizes to the bone and the lymph nodes. This uncertainty of the biology of the prostate cancer creates uncertainties on how to predict the outcome of the disease and therefore how to treat the disease.

Diagnostic Tools

The current diagnostic tools for prostate cancer are prostate specific antigen (PSA) test, Digital Rectal Examination (DRE), biopsy, and Gleason Score (Karakiewicz & Aprikian, 1998). The PSA test measures the antigen quantity in the blood serum and men with PSA levels between 4.0 and 10 ng/ml are a target population for prostate cancer (Jacobsen et al., 1995). Prostate cancer is a heterogeneous disease that is very commonly asymptomatic and thus identification of an increase in PSA levels can identify men with

prostate cancer who would otherwise not know (Jacobsen et al., 1995; Ellison et al., 2001). While raised serum PSA is a clinically adequate tumour marker, it is not specific to prostate cancer, thus it can result in false positives (Ellison et al., 2001). As mentioned above, the PSA test is partially responsible for the increase in incidence rate due to identification of prostate cancer in men with localized disease who were asymptomatic (Jacobsen et al., 1995). The PSA test was discovered in the 1980's and since this time the incidence rate has increased because asymptomatic men were diagnosed with prostate cancer. Once the disease is verified by biopsy, sections are graded by the Gleason Score which is the only critical test to help decide treatment options (Gomella et al., 2011). Due to PSA testing and Gleason scoring, the identification of early disease, the survival rate is near 100% (Ellison et al., 2001).

Treatment Options

As mentioned previously, prostate cancer usually grows very slowly and therefore has a low overall risk of turning into a clinically relevant disease, giving rise to the concepts, "watchful waiting" (Kasperzyk et al., 2011) and "active surveillance" (Gorin et al., 2011). These approaches are for "low risk" patients with a life expectancy of 20 years (Gorin et al., 2011). Radical prostatectomy, or removal of the prostate gland, has significant side effects which lowers the quality of life for the patient. The extraction of the entire gland creates an array of life altering complications such a urinary incontinence (Doherty & Almallah, 2011) and sexual dysfunction (Siegel et al., 2001). Taken together, surgery is not always the end result in this disease and there is evidence that

"active surveillance" can work without adding to the mortality rate (Graversen et al., 1990). On the other hand, there is a possibility that an aggressive cancer will be missed and the opportunity for a life-saving surgery. Despite the inherent advantages and disadvantages of "active surveillance" and radical prostatectomy (Bangma, 2011), it may be safer to intervene and treat the tumour with another means. An alternative therapy would be radiation therapy which is the use of ionizing x-ray beams to destroy the tumour cells. However, drawback of this therapy is exposure and degradation of healthy cells to ionizing radiation. Furthermore, chemotherapeutics are small molecule drugs which are toxic to all proliferating cells in the body and therefore subject the patient's healthy cells to significant toxicity. These harmful effects of chemotherapy result in unwanted side effects such as hair loss, nausea, and sexual and fertility dysfunction. Most chemotherapeutic drugs do not preferentially target the tumour and therefore subject the patient's healthy cells to significant toxicity. Radical prostatectomy and radiation is used for localized disease versus chemotherapy treatment for advanced prostate cancer (Bangma, 2011; Doherty & Almallah, 2011). No treatment currently available offers a clear survival advantage to patients with advanced prostate cancer, highlighting the urgent need for new targeted therapeutic strategies.

1.2 Liposomes as Therapy Vehicles

Liposomes were first described by Alec Bangham (1964) as spherical lipid particles comprised of a phospholipid bilayer enclosing an aqueous core (Bangham & Horne, 1964). Due to their intriguing inherent resemblances to cell membranes, liposomes are considered universal drug vehicles in the cosmetic and pharmaceutical industries (Drulis-Kawa & Dorotkiewicz-Jach, 2010). Liposomes have therefore gone through intense research and development to improve drug delivery. Both hydrophobic and hydrophilic active molecules can be encapsulated within the liposomal structure due to their unique architecture (Liautard et al., 1991). Hydrophobic molecules are located within the bilayer (Schwendener & Schott, 2010) whereas hydrophilic molecules are located in the core of the particle (Liautard et al., 1991). Liposomes are inert, biocompatible particles giving rise to the phenomenon of "drug vehicles" to improve the drug pharmacokinetics and bioavailability. The active molecules entrapped in the core can vary from small molecule drugs, antibiotics, nucleic acids, and peptides (Drulis-Kawa & Dorotkiewicz-Jach, 2010; Lutsiak et al., 2002; Uziely et al., 1995; Yagi et al., 2009). The unique ability to shield the cargo from degradative mechanisms in cells but to also protect healthy cells from toxic drugs within makes liposomes an attractive asset to therapeutic delivery (Kaye & Richardson, 1979; Mayer et al., 1989).

"Stealth" Liposomes

Decades of research, have been dedicated to improving the bioavailability and tumour uptake of liposomes. To improve the bioavailability, addition of polyethylene glycol polymer chain (PEG) molecules are covalently attached to liposomes. PEGylation protects the liposomes from detection of the immune system. The theory of Stealth ® liposomes were first introduced by Allen (Allen et al., 1992) and are considered the "second generation" of liposomal drug delivery (Immordino et al., 2006). Sterically stable liposomes increase the pharmacokinetics of the drug and sustain a longer blood circulation time (Allen & Hansen, 1991). PEGylated liposomes are currently in clinics to treat a variety of different cancers including breast, ovarian and prostate (Park, 2002), one such example is Doxorubicin encapsulated within PEGylated liposomes (commercial name: DOXIL) (Allen & Hansen, 1991). However, it was observed by Mishra et al that liposomes functionalized with PEG have been found to decrease endosomal escape resulting in degradation of the cargo (Mishra et al., 2004). While addition of PEG molecules to liposomes have a clear benefit on the systemic level, on a cellular level PEGylation poses a clear disadvantage (Remaut et al., 2007). For example, the therapeutic index of even these newer "second generation" formulations, is still quite low due to non-specific uptake and endocytosis-mediated drug degradation (Figure 1.1A). Despite the recent advancements of increasing the drug bioavailability and pharmacokinetics, there is still suboptimal delivery of the cargo to inside the cells.

1.3 "Fusogenic" Entities

"Fusogenic" Lipid

Another critical milestone in liposomal development was the introduction of fusogenic moieties to avoid endosomal degradation. Once liposomes are endocytosed, the particles are challenged by the acidic environment and thereby an escape mechanism is needed to salvage the cargo they carry. The simplest method is incorporation of a "fusogenic" lipid, such as a neutral helper lipid phosphatidylethanolamine (PE) (Farhood et al.,1995; Zhou & Huang, 1994). Several groups have shown that addition of 1, 2-dioleoyl-sn-glycerol-3 phosphatidylethanolamine (DOPE) in their liposomes will significantly increase the transfection of deoxyribonucleic acid (DNA) (Farhood et al., 1995; Zhou & Huang, 1994). Zhou and Huang reported the presence of DOPE increases the DNA transfection by 60% compared to liposomes without DOPE (Zhou & Huang, 1994). The authors also reported that the DNA entered the cytoplasm mainly by destabilizing endosomes and provoking endosomal escape (Zhou & Huang, 1994). Furthermore, Farhood et al demonstrated that this endosomal release was only in the presence of high levels of DOPE (Farhood et al., 1995). In extension of these studies, DOPE was characterized to have a cone-like structure which adopts a hexagonal phase that disrupts the endosomal membrane and initiating the escape into the cytoplasm (Zuhorn et al., 2005). Taken together, DOPE acts as an endosomolytic agent depositing the cargo into the cytosol of cells.

"Fusogenic" Peptides

Efforts have been made to mimic methods employed by viruses for intracellular delivery of macromolecules (Kobayashi et al., 2009). Studies have been reported using a variety of pH sensitive peptides such as vesicular stomatitis virus proteins, phage coat proteins proteins and shGALA to name a few (Peisajovich et al., 2002; Sakurai et al., 2011). These viruses have evolved as an effective strategy to escape the endosomal uptake of compounds by exploiting biological processes. There are many fusogenic peptides that can traffic membrane impermeable compounds into the cell by endocytosis, however only limited studies have been accomplished to incorporate these proteins within liposomes.

VSV G protein

Previous research has successfully reconstituted an enveloped viral protein, vesicular stomatitis virus (VSV) glycoprotein (G) protein within liposomes using Octylglucoside (OG) dialysis (Eidelman, 1984; Metsikko, 1986; Petri, 1979). Petri et al was the first to describe the insertion of the VSV G protein within a lipid bilayer using the OG detergent depletion. In extensions of this study, to evaluate the fusogenic capabilities, other groups discovered that the fusion was pH dependent (pK~4.0) and therefore the entry within endosomes was needed for the G protein to exert its effect (Eidelman et al., 1984). Furthermore, it was observed that, upon detergent dialysis using SM2 beads to remove the detergent, the G protein loses fusion activity (Metsikko et al., 1986). The authors speculate that the hydrophobic beads caused denaturation of the G protein (Metsikko et al., 1986). Despite these inherent advantages of rapid endosomal release, the key strategy

for improved efficiency of liposomal therapeutics would be to penetrate the cell membrane bypassing endocytosis.

Phage Coat Protein

Phage coat proteins are examples of fusion proteins which increase the intracellular escape from endosomes (Wang, et al., 2010). Recent studies, using a phage coat library technique, have identified PVIII protein with specific fusion abilities toward targeted cells (Jayanna et al., 2009). It was observed through fluorescence microscopy, that phage liposomes were taken up by endocytosis and triggered membrane fusion in the endosomal acidic environment (Wang et al., 2010). The authors compared their phage liposomes to plain liposomes and visualized the perinuclear punctuate localization of the standard liposomes compared to the diffuse distribution of the phage liposomes. The authors postulated that the diffuse pattern was a result of endosomal escape through fusion of the pH sensitive phage proteins to the endosome bilayer (Wang et al., 2010). Furthermore, they verified this theory by adding an endosome acidification inhibitor (NH_4CL) and observed the entrapment of the phage liposomes within perinuclear vesicles (Wang et al., 2010). Thereby, confirming the pH sensitive phage liposomes elicit their fusion capabilities in the acidic endosomal environment to release their cargo intracellularly. Despite the success of inserting these fusogenic peptides into liposomes, unsuccessful fusion with the cell membrane was observed. These endosomal release strategies using enveloped viruses increased the intracellular delivery compared to standard liposomes however, the results are sub-optimal and the ultimate goal of fusion with the cell membrane was not successful.

1.4 P14 Liposomes

Orthoreovirus Non-enveloped Fusion Proteins

Fusion associated small transmembrane (FAST) proteins are a unique class of proteins encoded by the genus orthoreoviruses. The five distinct species in the orthoreoviruses genera include the avian reovirus (ARV), nelson bay reovirus (NBV), and baboon reovirus (BBV), aquareovirus reovirus (AQV) and reptilian reovirus (RRV) (Duncan, Murphy, & Mirkovic, 1995; Duncan et al., 2004; Gard & Compans, 1970; Shmulevitz & Duncan, 2000). Reoviruses represent a distinct group of non-enveloped viruses that are capable of forming multinucleated cells, syncytia (Duncan et al., 1996; Duncan et al., 2004; Shmulevitz et al., 2003; Shmulevitz et al., 2004; Top et al., 2011). Fusogenic reoviruses are a rare exception of non-enveloped viruses which induce cell-cell fusion independent of virus entry and production (Duncan et al., 1996; Duncan, 1996; Shmulevitz & Duncan, 2000). A typical phenotype for enveloped viral proteins promotes entry of the virus into cells (Shmulevitz & Duncan, 2000). Upon infection of these reoviruses, fusion associated small transmembrane (FAST) proteins are translocated to the cell surface mediating cell-to-cell fusion (Shmulevitz & Duncan, 2000; Shmulevitz et al., 2002).

The classification of the reptilian reovirus was recorded by Duncan et al as a distinct species of the fusogenic reoviruses (Duncan et al., 2004). Even though the reptilian virus was discovered and isolated years before from a moribund python in 1987 (Ahne, Thomsen, & Winton, 1987), the virus was never classified as a new fusogenic species at that time. Duncan et al established the newly identified reovirus after confirming the virus induced extensive multi-nucleated cells (syncytium) in infected cell cultures typical

of fusogenic reoviruses. Furthermore, the 125 amino acid fusion protein had differential sequences compared to the other FAST proteins.

P14 FAST Protein Structure

The reptilian reovirus FAST protein was named according to the molecular weight in kDA, p14. The authors characterized the structural motifs of the p14 protein and revealed its own signature arrangement of a myristoylated N-terminus; however the protein remains surface-localized (Corcoran & Duncan, 2004). Figure 1.2 illustrates the structure of the p14 FAST protein, highlighting the N-terminal myristoylation site, the hydrophobic path, a single transmembrane domain, and the exposed C-terminus. Further studies indicated that the myristoylation of the N-terminal region was responsible for the fusion capabilities (Corcoran & Duncan, 2004; Corcoran et al., 2004). It was demonstrated that point mutations at the myristoylation site renders the p14 fusion incompetent (Corcoran et al., 2004). Moreover, to confirm the N-terminal myristoylation site was solely responsible for the fusion abilities, deletion of the C-terminal 10-20 amino acids was evaluated. Overall, the extent of fusion remained unaltered, however the rate of syncytium was slowed (Corcoran et al., 2004). Taken together these results confirm that the post translational modification of p14 is both functional and essential for fusion activity (Corcoran et al., 2004).

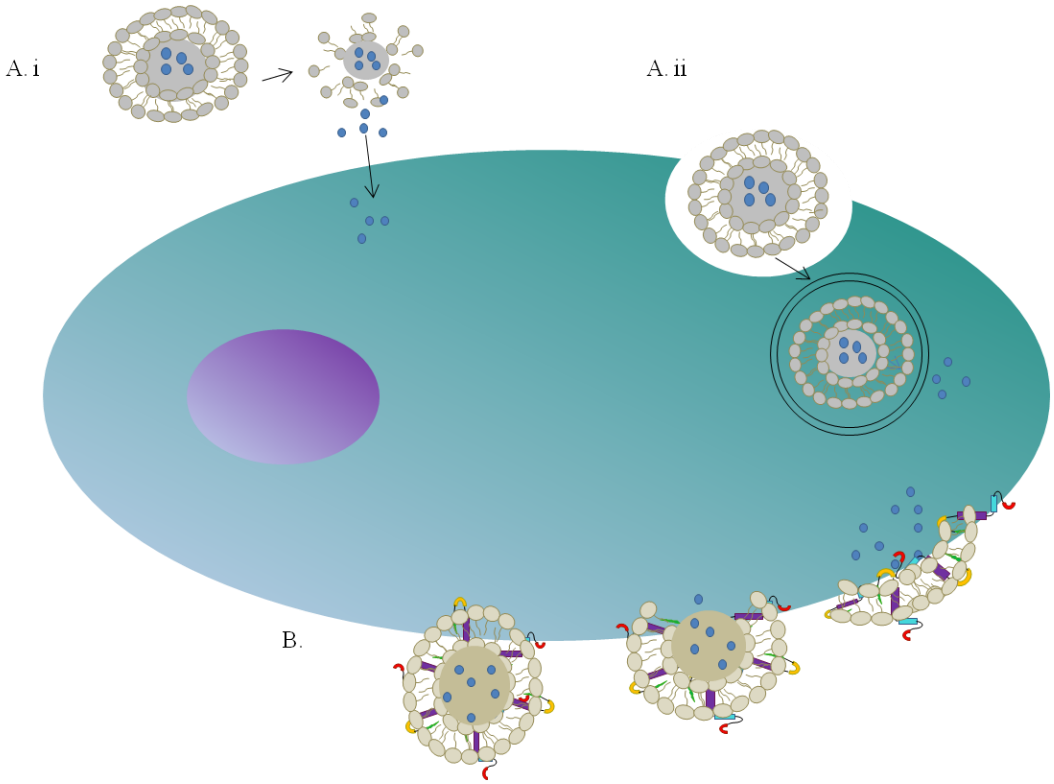

Figure 1.1 Representation of Intracellular Cargo Delivery Using Liposomes

A) *Standard liposomal* technology depends on two routes for intracellular delivery; i) non-specific leakage of the cargo out of the liposome and passive uptake by the target cells or ii) uptake of intact liposomes into the endosomal pathway.
B) *Fusogenic liposomes* include the p14 FAST protein which mediates efficient liposome-cell fusion, bypassing the endocytic pathway, depositing the cargo directly into the target cell. The fusogenic liposomes therefore have a distinct advantage over the standard liposomes when delivering cargo intracellularly.

P14 Reconstituted into Liposomes

In an extension of these studies, the authors tested whether p14 protein could function on its own to induce membrane fusion when reconstituted in liposomes (Top et al., 2005). The p14 protein was inserted into the artificial bilayer using OG detergent depletion method (Petri & Wagner, 1979). The authors identified the equal protein orientation by immunofluorescence staining of both the exposed N-and C-terminus (Top et al., 2005). The theory proposed by the authors is that exposure of the p14 N-terminal myristoylation on the surface of the liposomes allows the p14-liposomes to interact with cell membrane of target cells (Figure 1.1 B). Figure 1.1 demonstrates the comparison of cargo uptake between the standard and fusogenic liposomes. The successful intracellular delivery of the cargo using standard liposomes is based upon i) non-specific leakage of the encapsulated cargo in the bloodstream and passive uptake by the target cells and ii) uptake of the intact liposomes into the endosomal pathway (Figure 1.1A). The cargo contained within standard liposomes is prone to degradation upon entry into the endocytic pathway. For this reason, the standard liposomes are restricted to specific cargos that posses inherent membrane penetration capabilities and the ability to withstand the acidic environment of the endosomal pathway. However, it is hypothesized that fusogenic liposomes fuse with the cell membrane via the N-terminal myristoylation site allowing lipids from the cell membrane and liposomes to mix, for direct deposit into the cell (Figure 1.1B) (Top et al., 2005).

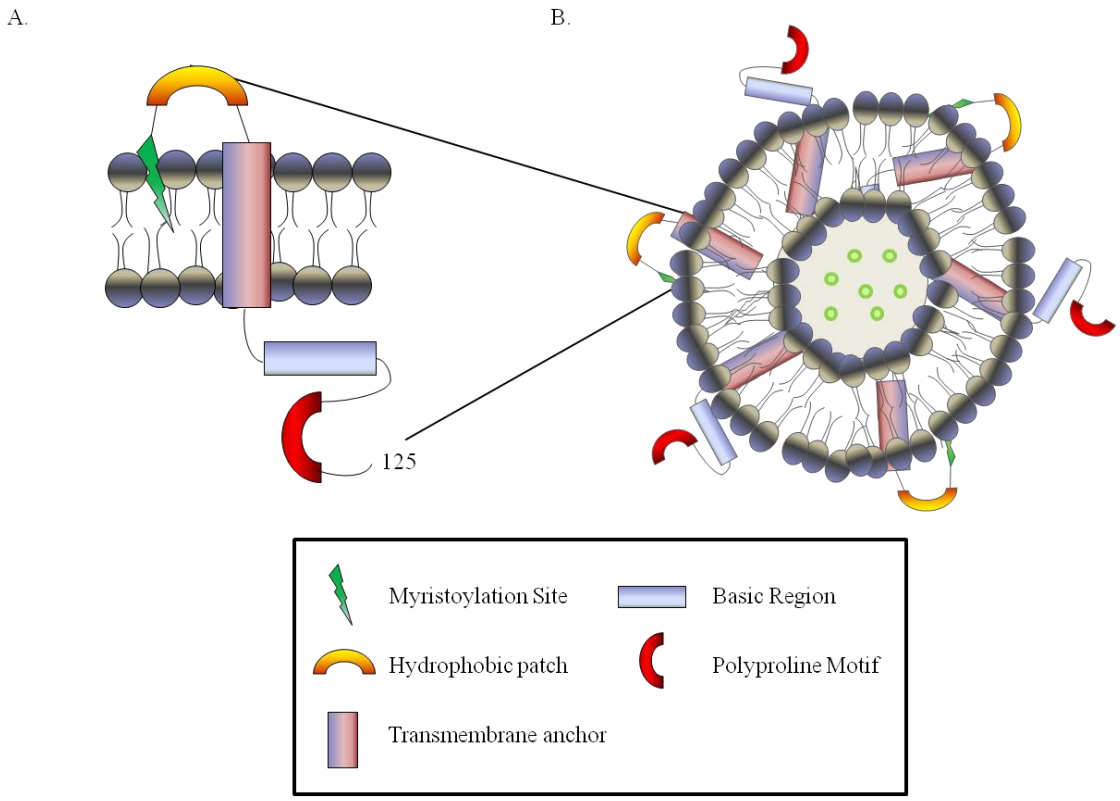

Figure 1.2 Schematic representing the fusogenic liposomal platform

A) The structure of p14 Fusion Associated Small Transmembrane (FAST) protein. The p14 protein is encoded by the reptilian reovirus (RRV) and is named according to the molecular weight in kDa. The 125 residue structure contains; N-terminus myristoylation site (green triangles), the hydrophobic patch (yellow half circle), transmembrane domain (purple rectangle), basic region (blue rectangle) and the C-terminus polyproline motif (red half circle). Reprinted from (Corcoran & Duncan, 2004; Top et al., 2005).
B) Representation of fusogenic liposomes; p14 spans the lipid bilayer displaying either the N- or C- terminus on the surface of the liposome. The green circles represents the "cargo" (example in this thesis: fluorescein isothiocyanate (FITC)) encapsulated within the core of the liposome.

P14 Induces Lipid Mixing with the Cell Membrane

To test the lipid mixing hypothesis, Top et al performed a FRET, (fluorescence resonance energy transfer) assay and measured the fluorescence by flow cytometry (Struck et al., 1981; Top et al., 2005). The increased cell fluorescence over time was observed with p14-liposomes whereas this increase was not observed with standard liposomes (Top et al., 2005). To ensure these results were due to lipid mixing, the authors added lysophosphatidylcholine, a monoacylated fatty acid known to inhibit membrane fusion (Chernomordik & Kozlov, 2003; Top et al., 2005). The addition of lysophosphatidylcholine efficiently inhibits lipid mixing of the p14-liposome and the cells, confirming the lipid mixing hypothesis (Top et al., 2005). The exceptional structural features of p14 initiate liposome-cell lipid mixing identifying a potential liposomal carrier which bypasses endocytosis.

P14 Liposomes Intracellular Delivery

Cytoplasmic delivery of therapeutics is highly desirable, however very difficult to achieve because poor performance of standard liposomes and previously described fusogenic peptides. The ideal delivery system would bypass the endocytic pathway and deliver the cargo directly to the cytosol of cells. The unique feature of the p14 FAST protein has the potential to solve this drug delivery caveat. Mader et al demonstrated the ability to deliver a cytotoxic peptide directly to the cell cytoplasm via p14-liposomes (Mader et al., 2007). Bovine lactoferricin (LfcinB) is a cationic peptide that kills leukemia cells. In the presence of endocytosis inhibitors, LfcinB on its own was not

internalized by receptor mediated endocytosis (Mader et al., 2007). However, when LfcinB was delivered using p14-liposomes, the release was directly into the cytosol causing cell death (Mader et al., 2007). The extensive studies on p14 and how it interacts within a lipid bilayer has given critical insight into a novel fusogenic liposome that does bypass endocytosis, however penetrates the cell membrane.

1.5 Passive Targeting

Another interesting property of liposomes is their natural ability to accumulate at the tumour site. Healthy, normal blood vessels are comprised of endothelial cells that are bound together by tight junctions and therefore inhibit large particles from leaking out of the vessel. Consequently, the tight junctions of tumour vessels are compromised and particles are able to leak through the leaky cell fenestrations. This process of passive targeting occurs because of the various anatomical anomalies that occur in tumour vessels, such as leaky vasculature and poor lymphatic drainage, termed enhanced permeability and retention effect (EPR) (Matsumura & Maeda, 1986). Matsumuri et al studied the EPR effect by testing the accumulation of macromolecules in tumour tissue upon intravenous injections of radioactive labeled protein in a mouse model (Matsumura & Maeda, 1986). The authors were able to identify the collection of labeled macromolecules in the subcutaneous tumours and concluded that the vasculature near the tumour had been compromised and these macromolecule accumulations were due to passive targeting of the EPR effect (Matsumura & Maeda, 1986). A key consideration for the design of nanocarriers to take full advantage of the EPR effect is the size of the particle (Yu et al., 2010). It was identified that particles of < 200 nm in diameter are the preferred size to rapidly accumulate at tumour sites via the EPR effect (Liu et al., 1992). Furthermore, PEGylated liposomes reduce the recognition by the RES and long circulating liposomes are required for extravasation (B. Yu et al., 2010).

Taken together, liposomes were shown to extravasate and accumulate selectively in tumour interstitium of a variety of murine models as a result of EPR effect. Figure 1.3 demonstrates the differences between liposome accumulations in tumour versus normal vasculature, highlighting the effects of the EPR effect. Therefore, liposomes could accumulate over time in solid tumours after intravenous administration. Moreover, current anti-cancer therapeutics, such as DOXIL®, are passively targeting tumours and by virtue of the EPR (Kuijpers et al., 2000). However, passive targeting cannot promote further uptake by cancer cells once they have arrived. Therefore, further investigation of targeted receptor mediated uptake would increase the therapeutic window of anti-cancer drugs.

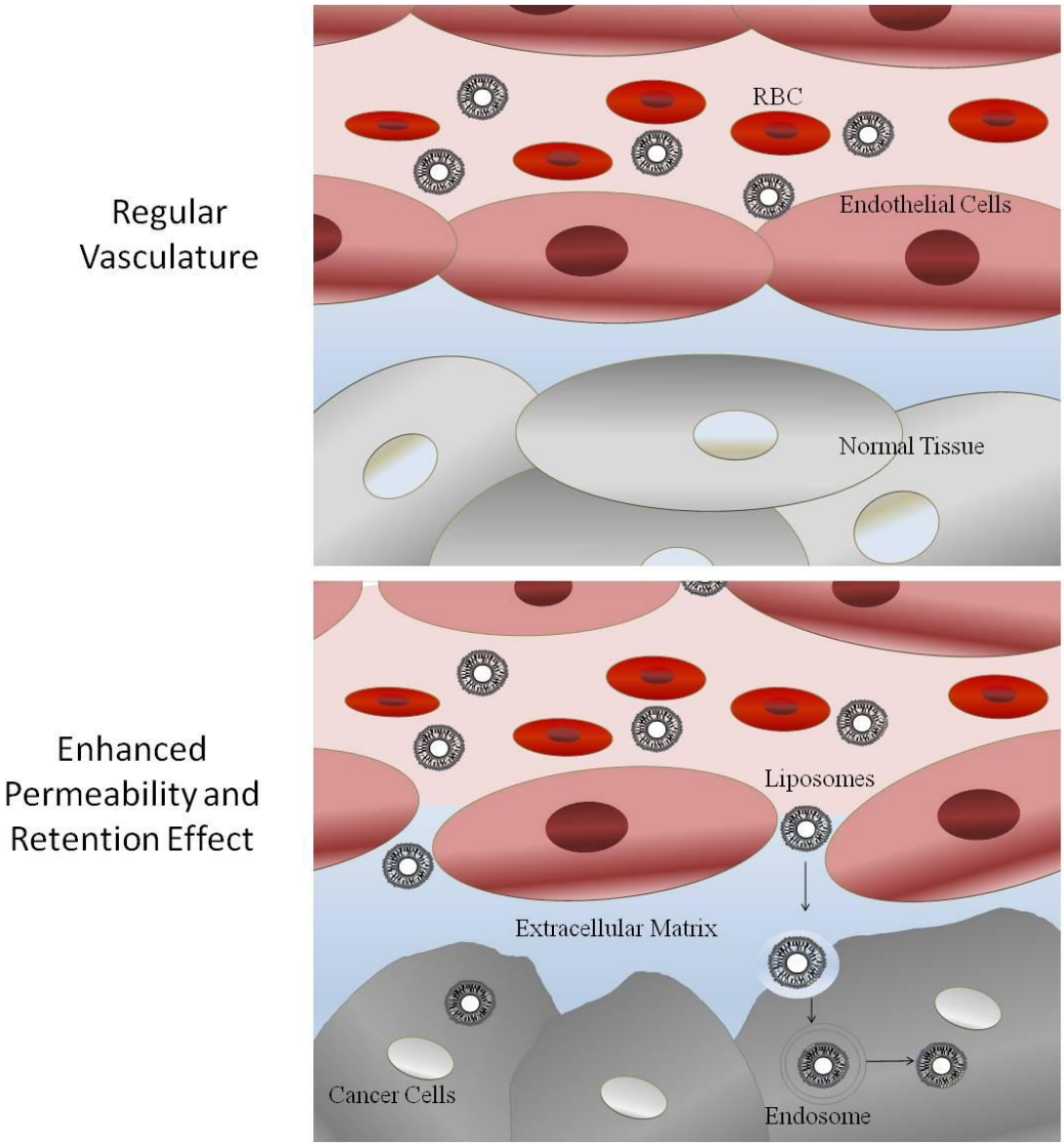

Figure 1.3 Schematic of the enhanced permeability and retention effect (EPR) Normal vasculature permits liposomes to pass between the endothelial cells, whereas the EPR effect results in leaky vasculature where liposomes <200 nm in diameter can pass between the junctions and act on the cancer cells.

1.6 Active Targeting

"Smart Particles" or "Magic Bullets" are terms coined for the phenomenon that therapeutics can selectively target and kill cells without harming the neighboring cells. Direct targeting of cancer cells using liposomes has the potential to treat cancer with higher efficiency than standard anti-cancer therapeutics. There are key points to consider when creating targeted nanoparticles; 1) a target should be in sufficient quantity (overexpressed) providing a good opportunity to bind to the target 2) ligand attachment should be attached to the surface of the particle and 3) a target should facilitate internalization (Maruyama, 2011).

Prostate Targeting Ligands

Direct targeting of prostate cancer is a strategy towards killing the cancerous cells while decreasing healthy bystander cell toxicity. Various types of targeting ligands have been exploited for directing liposomes to prostate cancer (Table 1.1). Attention has been directed towards targeting liposomes to cell integrins, as they have significant expression on tumour vasculature. Such peptides that would bind to αvβ3 and α5β1 integrins are promising ligands to target a variety of different cancers, including prostate (Arap et al., 1998; Demirgoz et al., 2008). Demirgoz et al examined the targeted efficiency of the PR_b functionalized liposomes to α5β1 integrins (Demirgoz et al., 2008). The authors demonstrated that liposomes functionalized with PR_b improved the cytotoxicity displayed by the total higher fluorescent intensity for prostate cells in stages of apoptosis (Demirgoz et al., 2008). Despite recent advancements with targeting the αvβ3 integrins

with RGD decorated liposomes, the studies using PR_b liposomes demonstrated a clear advantage over the RGD targeting techniques (Demirgoz et al., 2008). Other, attractive targets for cancer are the transferrin and folate receptors as they are both highly up regulated on tumours (Gabizon et al., 1999; Singh, 1999; W. Yu et al., 2004). While these ligands target a variety of different cancers, the anti-PSMA ligand is specific for prostate cancer. Expressed on the surface of prostate cancer cells, the prostate specific membrane antigen is used in targeted delivery. Ikegami et al constructed liposomes containing anti-PSMA for targeting gene therapy and concluded that the transfection was higher in the targeted liposomes than that of normal liposomes (Ikegami et al., 2006). There are many different targeted ligands that can be conjugated to the surface of liposomes; however, it is the method on which the ligand is supported that will prove to be efficient.

Table 1.1 Prostate Cancer Targeting Ligands for Liposomes

Type	Targeting Ligand	Receptor	References
Peptide	RGD PR_b	αvβ3 α5β1	(Arap et al., 1998) (Demirgoz et al., 2008)
Protein	Transferrin	Transferrin Receptor	(Singh, 1999; W. Yu et al., 2004)
Antibodies	Anti-PSMA	PSMA Receptor	(Ikegami et al., 2006)
Small Molecules	Folic Acid	Folate Receptor	(Gabizon et al., 1999)

Attachment of the Targeting ligand

The construction of a targeted particle requires the conjugation of the ligand to the surface of the liposomes. The two methods deployed for the attachment of ligands are either covalent or noncovalent coupling (Nobs et al., 2004). Ligands can either be assembled with phopholipid headgroups of non-PEGylated liposomes or can be anchored to the liposomes via PEGylated chains (Maruyama, 2002; Sofou, 2007). Different covalent coupling strategies include thioether bonds, disulfide linkage, crosslinking, and hydrazone bond (Hansen et al., 1995; Nobs et al., 2004). Despite these efforts to attach ligands to the surface of liposomes, there is not an optimal covalent coupling reaction. This is due to the drawbacks of the number of crucial parameters, such as the length, type and localization of the crosslinker. Covalent reactions also require chemical reagents which could potentially alter or damage the ligand or the liposome (Hansen et al., 1995). Non-covalent coupling is beneficial over covalent coupling because there is no need for harsh chemicals (Nobs et al., 2004). However, this method is not widely used because of the weak interaction of ligand on the liposomal surface (Duarte et al., 2011; Nobs et al., 2004). Therefore, targeted proteins that can be inserted into the bilayer of the liposomes would be optimal, due to these drawbacks of coupling to the surface of the liposomes.

1.7 Bombesin Targeting Peptide

The development of anti-cancer therapeutics that can be targeted to specific receptors, over-expressed in prostate cancer, but sparse the uptake in normal tissue, is critical. Receptors for the gastrin releasing peptide are over-expressed in several human tumours, including pancreatic, small lung carcinoma, breast, and prostate (Varvarigou et al., 2004). Originally isolated from the skin of the fire bellied frog *Bombina bombina*, Bombesin is a 14 amino acid peptide (Anastasi et al., 1971). Although the GRPR is frequently expressed by many tumour types there are three other bombesin receptor subtypes that bombesin binds to, NMB, BRS-3, and BB4 (Reubi et al., 2002). Furthermore, prostate cancer cells express approximately 48000 GRPR per cell (Aprikian et al., 1996). Many radiolabelled bombesin analogues have been created for SPECT and PET modalities to target the GRPR, allowing for novel prostate cancer imaging probes (Ananias et al., 2008; Safavy et al., 1997). Even though there have been no studies performed conjugating bombesin to liposomes there has been however, bombesin attachment to polymeric (Lee et al., 2010) and viral nanoparticles (Steinmetz et al., 2011). Current studies in our laboratory have demonstrated the tumour homing efficiency of bombesin virus particles by intravital imaging in a xenograft avian embryo model of human prostate cancer (Steinmetz et al., 2011). We validated bombesin targeting to a human prostate cancer cell line (PC3) *in vitro* by confocal microscopy. Non-targeted viral nanoparticles did not bind to PC3 cells at an appreciable level compared to bombesin particles (Steinmetz et al., 2011). To ensure that binding of the bombesin particles was specific for the GRPR a 10-fold excess of free bombesin peptide was added to block the particles, resulting in a dramatic decrease in bombesin-viral uptake (Steinmetz et al.,

2011). This previous research in our laboratory suggests that bombesin would be suitable for functionalizing liposomes to target prostate cancer.

1.8 Nucleic Acid Delivery Using Liposomes

Liposomes have been used as carriers for many different applications and are not limited by the cargo they carry. As mentioned previously, nucleic acids can also be packaged within liposomes to improve the delivery of deoxyribonucleic acid (DNA) and small interfering ribonucleic acid (siRNA). Traditional transfection reagents such as Lipofectamine™ are some of the most popular transfection reagents utilized for *in vitro* as they are comprised of a cationic lipid, 1-2, 3-dioleyloxy-propyl- trimethylammonium chloride (DOTMA) (Felgner et al., 1987). Cationic formulations facilitate the functional delivery into cells as they complex with the negatively charged nucleic acids. These traditional transfection reagents however, cannot be used *in vivo* because they are unstable in plasma and are eliminated rapidly from the blood. Consequently, neutral liposomes have been used instead. However, their encapsulation efficiency is low. Thus, the development of a liposomal carrier that provides physical containment of the nucleic acids is needed to overcome the problems associated with existing cationic carriers (Yagi et al., 2009).

Wrapped Liposomes

The development of novel liposomes "Wrapsomes" (WS) or "Wrapped Liposomes" (WL) were constructed using an innovative procedure (Yamauchi et al., 2006). The strategy was to increase the nucleic acid encapsulation efficiency by identifying an alternative liposomal formulation (Yamauchiet al., 2006). Complexes were prepared by incorporating a cationic lipid core in order to complex with the siRNA within a neutral

liposomal bilayer to increase the serum stability (Yamauchi et al., 2006). Yagi et al also adopted this unique lipid formulation and proved that WS nanoparticles stabilize siRNA decreasing the degradation in serum (Yagi et al., 2009). The authors also evaluated the WS uptake *in vivo* and reported inhibition of tumour growth (Yagi et al., 2009). Wrapped liposomes are the first to our knowledge to demonstrate efficient nucleic acid delivery *in vivo*.

Heparin Releases DNA from Liposomes

The strong interaction with cationic lipids to DNA creates difficulty when quantifying DNA encapsulation within liposomes (Gershon et al., 1993). Using conventional methods for quantifying DNA, such as Ethidium Bromide (EtBr), results in a decrease of intercalation because the cationic lipids displace the binding of the agent. In this vicinity, a compound needs to be added to substitute the lipids from the DNA before DNA quantification is performed. Addition of anionic polymers, such as heparin and dextran sulfate, is commonly used to displace the cationic lipids from the DNA (Tsai, Furstoss et al., 2002; Xu & Szoka, 1996; Zelphati & Szoka, 1996). Anionic polymers have a 2 fold greater charge density than DNA which explains why cationic lipids preferentially associate with the polymers over DNA and quantification can be performed (Casu, 1985). Previous studies demonstrated that heparin and dextran sulfate substantially released plasmid DNA (>50%) from cationic liposomes before quantifying with EtBr (Xu & Szoka, 1996; Zelphati & Szoka, 1996).

1.9 Hypothesis and Objectives

Given the structure of p14, we hypothesize that the incorporation of bombesin targeting peptide will be tolerated at the C-terminal end of p14, so that liposomes with cell-specific and fusogenic properties will increase the intracellular delivery of therapeutics and specificity for prostate cancer.

In this dissertation my objectives are as follows:

1) Establish the intracellular delivery of liposomes formulated with p14 protein (non-targeted)

a) Calculate the syncytia index of p14 expression in human fibrosarcoma (HT1080) cells

b) Determine the p14 localization in syncytium formation

c) Verify the fusogenic liposome platform by comparing the intracellular delivery of FITC compared to standard liposomes in human breast cancer (MDA-MB 231), human fibrosarcoma (HT1080), and prostate cancer (PC3) cells

2) Create a targeted fusogenic protein by conjugating bombesin to the C-terminus of the p14 to target the gastrin releasing peptide receptor overexpressed on prostate cancer

a) Generate a p14-bombesin plasmid and test the functionality using a fusion assay

c) Create a recombinant baculovirus to purify the p14-bombesin protein and verify the active protein

3) Assemble p14-bombesin liposomes and assess the delivery of fluorescein isothiocyanate (FITC) to prostate cancer cells

a) Insertion of the active proteins and test the uptake of the targeted liposomes on PC3 cells

4) Evaluate the specificity of the targeted fusogenic liposomes

a) Evaluate the uptake of p14-bombesin liposomes on benign prostatic hyperplasia (BPH) cells

b) Receptor blocking analysis

c) Knockdown of the GRPR using siRNA

5) Evaluate the intracellular delivery of nucleic acids

a) Encapsulate plasmid DNA using a novel wrapped liposomes carrier

b) Calculate the entrapment efficiency of the DNA within the WS

b) Assess the transfection efficiency of the p14-wrapsomes containing GFP

The preliminary results from the targeted fusogenic liposomes developed here indicate the novelty and the specificity of this therapeutic vehicle for prostate cancer. Although the data is ongoing, it provides a basis for a therapeutic carrier with the ability to increase the therapeutic efficacy of small molecule drugs and nucleic acids. The efforts made here contribute to the overall goal to deliver therapeutics to prostate cancer using the platform

developed in this dissertation. The fifth objective was to establish the efficacy of nucleic acid delivery. However, the results for plasmid DNA delivery are preliminary and the sample size is small. The data included in this thesis is a means to show the potential of such a platform for different uses.

Chapter 2

2 Materials and Methods

Cell culture

Spodoptera frugiperda insect cells (sf21) purchased from ATCC were grown in either a monolayer or in suspension. Adherent sf21 cells were grown in Graces 1x media (Gibco) supplemented with 10% fetal bovine serum (FBS) (Multicell), L-Glutamine (Multicell) and 10, 000 IU/ml penicillin and streptomycin (Invitrogen) at 27 ^{o}C. The suspension sf21 cells were grown in SFII 900 (Gibco) media supplemented with 3% FBS at 27 ^{o}C and rotated at 127 RPM. All of the following cells were purchased from ATCC; MDA-MB 231 Breast Cancer, Human Fibrosarcoma (HT1080) and HT1080 cell stably transfected with td-tomato (HT1080td-tom), and Prostate Cancer (PC3). MDA-MB 231 and HT1080/td-tom were grown in a monolayer with Dulbecco's Modified Eagle's Medium (DMEM) (Multicell) and PC3 cells were grown in F12K media (Multicell). The above medium was supplemented with 10% FBS and 10, 000 IU/ml penicillin and streptomycin and incubated at 37^{o}C in a humidified 5% CO_2 atmosphere. Benign Prostatic Hyperplasia (BPH) cells were a generous gift from Dr. Michael Cox, VGH) were grown as monolayers in low FBS 5% DMEM in the same conditions as the MDA-MB 231, HT1080 and PC3 cells. Quail Fibrosarcoma Muscle cells (QM5) cells were isolated and cultured in M199 media as described by Tran *et al.,* (Tran et al., 2009).

Antibodies

The following antibodies were used in this study: β tubulin mouse mAb (SIGMA), Gastrin Releasing Peptide Receptor (GRPR) rabbit mAb (Abcam), and p14 rabbit mAb (a gift from Dr. Roy Duncan's lab).

Western Blot Analysis

For analysis of GRPR, 80% confluent cultures of PC3, PC3 knockdown and BPH cells in 6 well plates were washed twice with 1x phosphate buffered solution (PBS) and detached from the dish with a sterile cell scraper. Samples were collected into microcentrifuge tubes and centrifuged at 14000 rpm for 5 minutes and then lysed with cold NP40 lysis buffer (1 % NP-40, 50mM Tris-HCL, pH 8.0, 150 mM NaCl) containing protease inhibitor cocktail (Roche) for 10 minutes on ice, centrifuged for another 14000 rpm for 10 minutes. Protein was collected and the concentrations were measured by the Bradford protein assay (BioRad). 10 µg of total protein was denatured in DL-Dithiothreitol (DTT) (Sigma-Aldrich) at 95^{o}C for 5 min and was loaded into 12 % gels, separated using SDS-PAGE gels and transferred to a polyvinylidene difluoride (PVDF) membrane (GE Healthcare). Membranes were blocked for1hr at room temperature in 5% skim milk (Bioshop) in TBST (10mM Tris base pH 7.4, 150mM NaCl, and 0.1% Tween 20). To probe for rabbit GRPR pAb (1:500), the rabbit p14 pAb (1:1000) or mouse β tubulin mAb (1:1000) in 5% skim milk in TBST was placed on the membrane overnight at 4^{o}C. After three washes of TBST, horseradish peroxidase conjugated secondary antibody, either anti-rabbit or anti-mouse (1:10,000 in 5% skim milk in TBST) (GE Healthcare)

was incubated1hr at room temperature followed by five washes with TBST. The presence of protein was evidenced by using the enhanced chemiluminescence (ECL) detection kit (GE Healthcare). All bands were quantified by densitometry using Image J gen analysis took and expression was reported relative to Tubulin expression.

Creation of recombinant p14-bombesin

A recombinant baculovirus encoding p14-bombesin was created using the Bac-To-Bac Baculovirus Cloning and Expression System (Invitrogen). Bombesin was cloned into the pFastBac1-p14 (generous gift from Roy Duncan (Top et al., 2005) transfer vector by PCR amplification under the control of the polyhedrin promoter between the restriction enzyme (RE) cleavage sites BamH1 and Xho1 (NEB). The following primers (Forward: 5'-GCGGATCCATGGGGAGTGGACCCTCTAATTTCG - 3'; Reverse: 5'-GCCTCGAGTTACATCAAGTGACCCACTGCCCAACTGATTCCCCAGCCTCTGCTCGTGATGGTGGTGATGGTGCTTGTTCGTCGTCATC-3') purchased from Sigma was incorporated an in-frame enterokinase-cleavable C-terminal 6x histidine tag, the entire bombesin sequence, and restriction sites for BamH1 and Xho1 into the PCR product for insertion into pFastBac1-p14. After purification (Bio Basic Inc. Gel extraction and PCR product purification kits) and enzymatic digestion with BamH1 and XHO1 (NEB), the construct was ligated into pFastBac plasmid under the control of the polyhedrin (PP) promoter, sequenced and transiently expressed into HT1080 cells. The sequences were confirmed by DNA sequencing analysis at Robarts Research Institute.

Plasmid Fusion Assay

HT1080td-tom and QM5 cells were seeded in 12 well plates to 70-80% confluency in DMEM and M199 media containing 10% FBS for 24 hours. The pFastBac-p14 and pFastBac-p14-bombesin were incubated with Lipofectamine 2000 (Invitrogen) as recommended by the manufacturer and added to cells in a ratio of 1 µg of DNA: 2 µl of Lipofectamine 2000 in serum free conditions and incubated at 37^{o}C. After 4 hours media was replaced with serum containing DMEM and M199. At the 8-10 hour time point the HT1080td-tom cells were analyzed using fluorescent microscopy. The QM5 cells were stained with CellTracker™ Green (Invitrogen) following manufacture guidelines and visualized using epifluorescence microscopy. The QM5 cells were also analyzed using a flow cytometry (Union Biometric) and staining the nuclei with SYTOX® green. The QM5 cells were detached from the surface using trypsin (Gibco) and cell suspensions were centrifuged for 1400 rpm for 5 minutes. Cell pellets were resuspended in 1X PBS, centrifuged for another 1400 rpm for 5 minutes before cells were fixed using 4% formaldehyde (Bioshop) solution in 1X phosphate buffered solution (PBS) for 10 minutes on ice. Fixed cells were centrifuged for 5 min at 1400 rpm. The fixative solution was then discarded and the pellet was washed 2x with 1X PBS. The cell pellet was stained using SYTOX® green (Invitrogen) according to manufacturing guidelines. The cell pellet was resuspended in PBS + 2% FBS and analyzed using flow cytometry.

Recombinant p14-bombesin Baculovirus

Following the Invitrogen's Bac-to Bac Baculovirus Expression systems, DH10αBac *Escherichia coli* (*E.coli*) (Invitrogen) cells contain a baculovirus shuttle vector (bacmid). Site-specific transposition of the pFastBac1-p14- bombesin expression cassette into the bacmid creates a recombinant baculovirus that was isolated from *E.coli* using standard mini-prep kit (Qiagen), and subjected to (0.5%) agarose gel electrophoresis for 1-2 hours at 125 volts. PCR analysis of the transposition region of the recombinant bacmid using M13/pUC forward and reverse primers (Life Technologies) was used to confirm insertion of the p14-bombesin open reading frame. The mini-prep p14-bombesin bacmid DNA and Cellfectin® (Life Technologies) in sf21were used to transfect 4 x 10^6 sf21 cells for 5 hours at 27 °C. The transfection medium was removed and replaced with sf21 supplemented with 10% (FBS). After 3 days at 27 °C, the recombinant baculovirus-containing supernatant was harvested and passaged 3 times in Sf21 cells.

Plaque Assay

The recombinant p14-bombesin baculovirus titer was obtained by the plaque assay following the Bac-to-Bac recombinant guidelines (Invitrogen). The plaque assay is used to determine the viral titer as plaque forming units per ml (pfu/ml), in order to determine the amount of virus used to infect insect cells for protein production. Healthy (>95 % viable) adherent sf 21 cells were seeded in 6 well plates (2 x 10^6 cells) and allowed to adhere for 1hr. Cell monolayers were infected with viral serial dilutions of low ratio p14-bombesin virus and an overlay of agarose medium mixture (Grace's 2x Insect media

(Gibco), 10% FBS and low grade 4% agarose (Bioshop)) was added to the monolayers to keep the cells stable and limits the spread of virus. Once the agarose medium has solidified, plates were placed in a humidified chamber for 5-10 days. Plaques (or clearings in the monolayer were visualized by inverting the plates. When an infected cell produces virus it eventually lyses and thus only adjacent cells become infected. Each group of infected cells is called a plaque, or a clearing in the monolayer of sf21 cells. Each plaque represents a single virus and thus the virus can be counted to determine the viral titer (pfu/ml) of the virus stock.

Protein Purification

Sf21 cells were grown in 3L suspension cultures to a cell density of approximately 4 x 10^6/ml and then infected with recombinant baculovirus at a MOI of 0.05 to 2.0, and shaken 127 RPM. At 24 or 48 h post-infection (~20% dead cells), infected cells were harvested and centrifuged at 150 x g for 20 minutes at room temperature. The resulting cell pellet was lysed with extraction buffer (50 mM sodium phosphate, 300 mM NaCl, 1.6% Igepal, and pH 7.0) plus protease inhibitors (200 nM aprotinin, 1 μM leupeptin, and 1 μM pepstatin). Insoluble debris was pelleted and the supernatant, containing p14 or p14-bombesin, was then added to TALON® Metal Affinity Resin (Clontech) and shaken gently for 3 hours at 4^o C for initial purification. The resin was washed with extraction buffer twice to remove unbound protein and the p14 or p14-bombesin was eluted from the resin with elution buffer (50 mM sodium phosphate, 300 mM NaCl, 150 mM imidazole, 1.6% Igepal, pH 7.0). The elute was dialyzed against 50 mM HEPES, 150mM

NaCl, 1.6% Igepal, pH 7.0) at 4 ^{o}C for 12 h and further purified using HiTrap SP HP (Sepharose High Performance column) (GE Healthcare) ion exchange columns (Amersham Pharmacia Biotech). The column was washed with four different buffers; Buffer 1 (50 mM HEPES, 185 mM NaCl, 1.6% Igepal, pH 6.8), Buffer 2 (50 mM HEPES, 1 M NaCl, 1.6% Igepal, pH 6.8), Buffer 3 (50 mM HEPES, 185 mM NaCl, 1.6% Igepal, pH6.8), Buffer 4 (50mM HEPES, 185 mM NaCl, 1.6% OG, pH 6.8). The p14 or p14-bombesin proteins were eluted from the column using 50 mM HEPES, 300 mM NaCl (or 450 mM for p14), 1.6% OG. The p14 or p14-bombesin concentration was determined by the BIO-RAD DC protein assay (BIO-RAD) and routinely adjusted to approximately 1 to 1. 5 mg/ml. The purity of the proteins and N-terminal myristoylation was estimated by sodium dodecyl sulfate-polyacrylamide gel electrophoresis (SDS-PAGE) using silver stained 12% polyacrylamide gels.

Protein Fusion Assay

The QM5 cells were seeded at approximately 80% confluency in a 12 well plates and allowed to adhere overnight. 4 µg of purified protein (p14 and p14-bombesin) was delivered using 3µl Lipofectamine (Invitrogen) for 4 hours in serum free conditions. The media was replaced with fresh supplemented media and incubated for 4 hours till the assay is complete. The syncytia formation was visualized in a similar technique as the vector fusion assay using CellTracker™ Green.

Assembly of Liposomes

All lipids were purchased from Avanti Polar Lipids Inc.; 1, 2-dioleoyl-sn-glycerol-3 phosphatidylcholine (DOPC), 1, 2-dioleoyl-sn-glycerol-3 phosphatidylethanolamine (DOPE), dimethylaminoethane-carbamoyl cholesterol (DC-chol) and cholesterol (chol). Liposomes were prepared by mixing lipids dissolved in chloroform DOPC: DOPE: DC-chol: chol, molar ratios of 60:30:4:6 in a round bottom flask with glass beads. Small glass beads were added to ensure even distribution of the lipid film upon rotary evaporation. The chloroform was evaporated for 1-2 hours using a vacuum with a rotary evaporator devise (Buchi). The lipid film was rehydrated with 1X PBS or 10 000 MW 1mg/ml fluorescein isothiocyanate (FITC) (Sigma) diluted in 1X PBS and added to the lipid thin film and vigorous shaking (2700rpm) for 1 hour at room temperature.

Sizing

The Avestin® extrusion apparatus is assembled and washed with methanol to dissolve any residual lipids and washed extensively with 1X PBS. To reduce the particle size the liposome emulsion is passed back and forth between the two Hamilton syringes containing polycarbonate filters (100nm pore size) 21 times. Sonication uses sonic energy to disrupt liposome emulsions into single membrane liposomes with diameters 90-120 nm. Liposome diameter was determined by dynamic light scattering (DLS) and ranged from 90-140 nm. Liposomes were stored at 4^{o}C and were used within two weeks.

Proteoliposome Preparation

For a 1 mL liposome preparation we insert 350 μg of purified protein into 20 mM liposomes (pre-extruded to 100nm using the Avestin Extrusion apparatus) using a detergent depletion method. The purified protein is reconstituted into the liposomes by mixing equal volumes of n-Octyl b-D-glucopyranoside (OG) (Bioshop) with the protein and the liposomes. The mixture was rocked for 45 minutes at 4°C. The OG was removed with overnight dialyses at 4^{o}C (18000 MW cutoff) with 3 changes of PBS and Bio-Beads SM-2 Absorbent (BioShop) to remove the residual detergent.

Liposome Uptake Studies

MDA-231, HT1080, PC3, and BPH cells were plated at 80% confluency in 6 well plates and grown overnight. The cell monolayer was replaced with cold PBS and cooled to 4^{o}C for 15 min. The liposomes were incubated on the cells (1mM) at 4^{o}C for 60 min. After 60 min incubation, the cells were washed with PBS and pre-warmed (37^{o}C) for 60 min to initiate delivery of liposomal cargo. After 60 min, the cells were collected and analyzed depending on the application.

Receptor Blocking

PC3 cells were incubated with excess free bombesin peptide (Purified in Dr. Len Luyt Chemistry lab) 10 min before the liposomal treatments on cells.

siRNA

Dharmacon predesigned sequence for the gastrin releasing peptide receptor (GRPR) small interfering RNA (siRNA) was purchased. 20 nM GRPR siRNA was transfected with jetPRIME™ (Polyplus) following manufacturer guidelines. The scrambled siRNA used as a negative control siRNA was purchased from Qiagen.

Wrapsomes

1, 2-dioleoyl-3-trimethylammonium-propane (DOTAP) lipid (~5.6 mM concentration determined by the calculation in Appendix B) purchased from Avanti Lipids was added to a round bottom flask with 400 µl of chloroform and small glass beads were added to ensure even distribution of the lipid film upon rotary evaporation. The chloroform was evaporated for 1-2 hours using a vacuum with a rotary evaporator devise. The lipid film was rehydrated with 100-500 µg of pcDNA 3.1-GFP (Midi-prep quality DNA) diluted in 1X PBS to a final volume of 1ml and vigorous shaking (2700rpm) for 1 hour at room temperature. The DOTAP-DNA core was then added during the hydration step of the assembly of liposomes described above and the same insertion protocol was used to reconstitute p14 protein within the bilayer.

Quantification of DNA Encapsulation

DNA encapsulation of pcDNA 3.1-GFP in WS was determined using the Quant-iT™ Pico green® ds DNA kit (Invitrogen) following manufacturer guidelines. Heparin

sodium salt (Bioshop) was also added to dissociate the DNA from the DOTAP core in order for the Pico green® to stain the DNA. Using the microplate protocol the samples were excited at 480 nm and the fluorescence emission intensity was measured at 520 nm using a spectrofluorometer.

Wrapsome Transfection

Human fibrosarcoma (HT1080) cells were seeded in 12 well plates at 60% confluency and allowed to adhere over night. 1 µg of standard and p14-wrapsomes pcDNA 3.1-GFP were incubated on the cells while Lipofectamine™ was used as a positive control.

Flow Cytometry

After liposomal treatment, the cells were detached from the surface using trypsin and cell suspensions were centrifuged for 1400 rpm for 5 minutes. Cell pellets were resuspended in 1X PBS, centrifuged for another 1400 rpm for 5 minutes before cells were fixed using 4% formaldehyde solution in 1X PBS for 10 minutes on ice. Fixed cells were centrifuged for 5 min at 1400 rpm. The fixative solution was then discarded and the pellet was washed 2x with 1X PBS. The cell pellet was resuspended in PBS + 2% FBS and analyzed using flow cytometry (Union Biometrica Biosorter).

Confocal Microscopy

The cells were seeded onto glass coverslips at a confluency of 80% and incubated with liposomes with the above cargo uptake studies. The cells were washed and fixed with 4% formaldehyde solution in PBS for 10 minutes at room temperature. After 2-3 washes with PBS, the cells were incubated one hour at room temperature with PBS- 1% BSA with or without 0.1% Triton X-100 (BioShop) depending on the need for intact membranes. Nuclear staining with DAPI and actin filaments stained with phalloidin. Confocal images were taken using 20x objective or an oil 63x objective in a spinning-disk confocal microscope, using a specialized instrument (Quorum Technologies) comprised of an upright Zeiss Axio Examiner Z1, LUDL filter wheels and large format motorized stage, a Yokogawa spinning disk head and a Hamamatsu 9100–12 Image EM CCD camera, controlled by Volocity (Improvision). Fluorescence images were further processed and analyzed using Volocity.

Statistical Analysis

All statistical analysis was performed in GraphPad Prism® with One-Way ANOVA and Tukey's multiple comparisons post-test with a statistical significance $p<0.05$.

Chapter 3

3 Results

3.1 Objective 1: Evaluation of Intracellular Delivery of Fusogenic Liposomes Formulated with p14-protein (non-targeted)

A syncytia assay of pFastBac-p14 in human cancer cells reveals cell membrane expression of p14 which induces cell to cell fusion in HT1080 cells comparable to Vero and QM5 cells previously examined

Calculation of the syncytial index in a time course fusion assay in HT1080 cells

Prior to developing a targeted fusogenic liposome, testing needed to be complete to verify previous studies and to establish standard assays with the native p14 protein. Preceding comprehensive studies characterizing the expression of p14 was successfully conducted in Vero and Quail Fibrosarcoma (QM5) cells (Corcoran & Duncan, 2004; Duncan et al., 2004). Vero cells were originally isolated from kidney epithelial cells from the African green monkey and are commonly used as host cells for growing viruses (Ito et al., 1964). Furthermore, QM5 cells lines are one of the preferred cell lines used in the propagation of avian reovirus dissemination (Tran et al., 2009). Duncan et al used Vero and QM5 cells when studying the propagation of the reptilian reovirus, discovering multinucleated cell formation (syncytia) similarly found with the avian reovirus (Duncan et al., 1996; Duncan et al., 2004). Our first aim was to determine if this phenomenon would occur if we transfected a plasmid containing the p14 sequence, pFastBac-p14 (generous gift from Dr. Roy Duncan), in a human cancer cell line. In this study, we discovered that expression of p14 in human fibrosarcoma td-tomato (HT1080td-tom) cells also induces

syncytia formation comparable to the results Duncan et al demonstrated in Vero and QM5 cells (Figure 3.1A) (Duncan et al., 1996; Duncan et al., 2004). The fluorescent microscopy images detail syncytial formation arises at 8hr post transfection (Figure 3.1 A&B). The results from Figure 3.1A demonstrate that the rate of syncytia formation is 8-10 hrs and figure 3.1B is a quantification of the syncytia formation using a manual cell counting approach. By staining the nuclei with DAPI and using a cell line that stably expresses a red fluorescent protein (Td-Tomato), we were able to count the number of nuclei per syncytium in five random fields of view to determine the number of nuclei present in syncytium.

P14 is a responsible for syncytia formation and is surface localized

To ensure p14 expression is responsible for the cell to cell fusion, immunostaining of permeabilized p14-transfected cells revealed numerous punctate regions radiating out to the plasma membrane. A p14 polyclonal antibody was used to stain the cells and antibody distribution was detected by immunofluorescence microscopy using an Alexa Fluor 488 secondary antibody (Figure 3.1 C). The p14 distribution had high fluorescence signal at the cell surface confirming membrane localization of p14 was responsible for the fusion of the HT1080 cells resulting in the syncytia formation (Figure 3.1 C).

These results in HT1080 cells are consistent with previous research in Vero and QM5 cells confirming that p14 is localized at the cell membrane to induce cell-to-cell fusion creating multinucleated cells *in vitro* (Corcoran & Duncan, 2004). The rate of syncytium formation, however, differs in HT1080 cells. Corcoran et al demonstrated significant

syncytia at 6 hr (Corcoran & Duncan, 2004) whereas we demonstrated significant syncytia at 8 hr post transfection. These findings establish a fusion assay suitable for HT1080 cells to test p14 FAST protein expressions and evaluate if the p14 is fusion active.

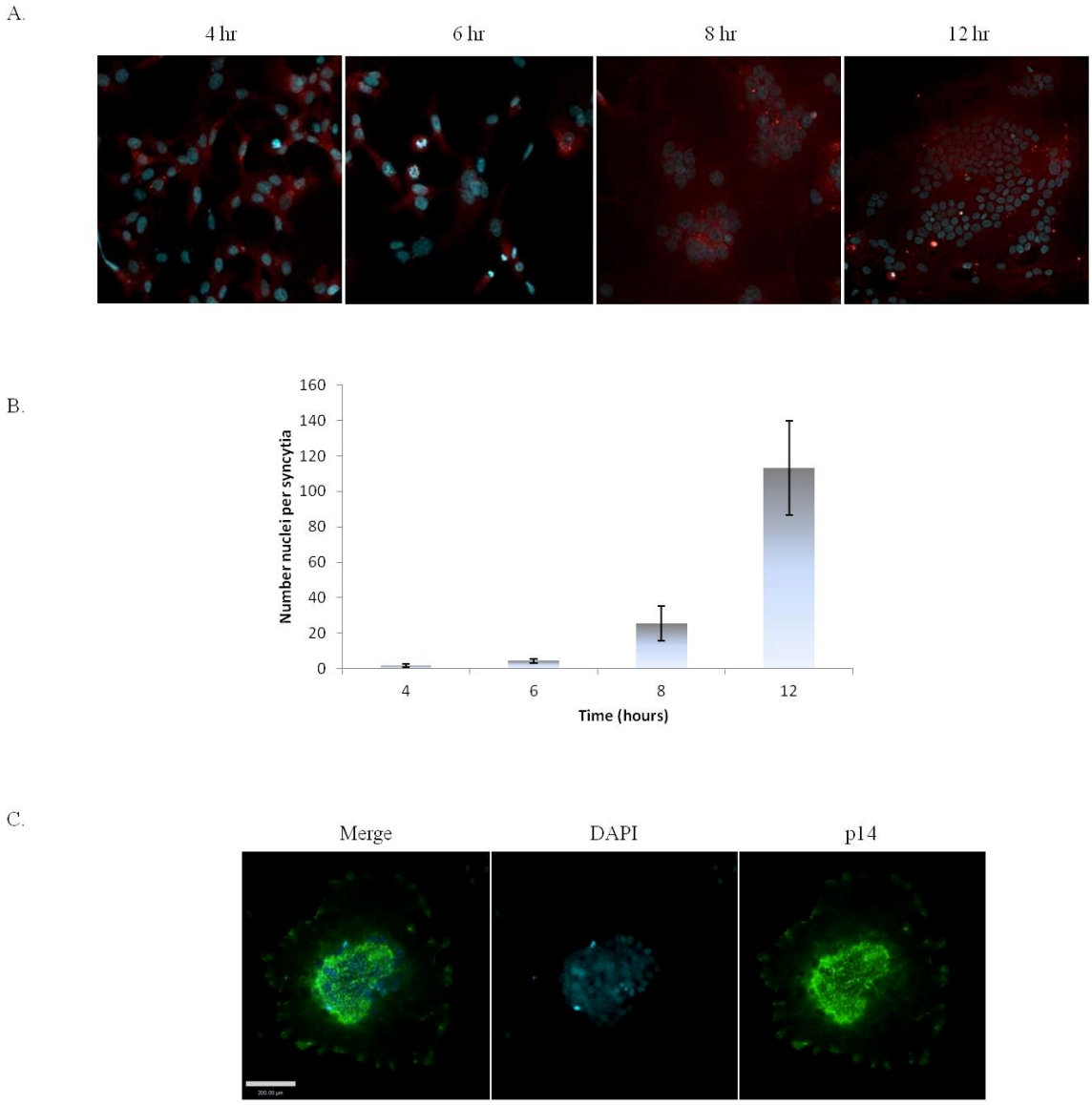

Figure 3.1 Expression of p14 plasmid creates multinucleated cells (syncytia).
A) Representative images of HT1080-td-tom cells, 4, 6, 8, 12 hr following transfection of pFastBac-p14. The nucleus was stained with a nuclear stain (DAPI) in order to identify the number of nuclei per cell (Magnification 20 x).
B) Quantification of the number of nuclei per syncytia as measured by manual counting of the nuclear signal (DAPI) within the HT1080-td-tom cell in the fluorescent images (5 fields of view). Syncytia formation was significantly visible after 8hr post transfection. This data is representative of n=2 experiment and results reported as the standard means $\pm$ standard error.
C) Immunofluorescent staining of permeabilized HT1080 syncytium 8 hr post transfection of pFastBac-p14 using a primary p14 antibody followed by an Alex Fluor secondary 488 antibody. The nuclei were stained with DAPI. The antibody distribution was detected by immunofluorescent microscopy and the antibody staining revealed intracellular p14 distribution and surface expression.

The Insertion of a Fusion Associated Small Transmembrane (FAST) protein into an artificial bilayer by detergent depletion method

Our initial investigation was to confirm the intracellular efficacy of fusogenic (p14) liposomes compared to standard liposomes (no protein). Prior studies documented that proteoliposomes containing the p14 (FAST) protein mediated liposome-cell fusion thereby increasing cytoplasmic delivery independent of endocytosis (Top et al., 2005). We utilized the liposome assembly protocol adapted by the Duncan laboratory, with a lipid profile containing 1, 2-dioleoyl-sn-glycerol-3 phosphatidylcholine (DOPC), 1, 2-dioleoyl-sn-glycerol-3 phosphatidylethanolamine (DOPE), dimethylaminoethane-carbamoyl cholesterol (DC-chol) and cholesterol (chol) in molar ratios of 60:30:4:6 (Table 3.1) (Top et al., 2005). The phospholipid composition has significant influence on the bilayer fluidity and therefore an appropriate lipid formulation is used to support the insertion of p14 (Cladera et al., 1997; Coderch et al., 2000; Top et al., 2005). Ensuring our liposomes resemble cell membranes as closely as possible we include cholesterol, a steroid commonly found in biological membranes (Coderch et al., 2000). Many proteoliposomes are assembled by covalent coupling of the protein to the liposomes surface which requires harsh chemicals. However, the insertion of this transmembrane protein requires the addition of a detergent to solubilize the protein (Lichtenberg et al., 1983; Paternostre et al., 1988). The purified protein was reconstituted into ~100 nm diameter liposomes by mixing 0.9 % OG (Appendix A) suspended p14 with liposomes presaturated with OG (Cladera et al., 1997; Petri & Wagner, 1979) followed by removal of the detergent. To ensure elimination of the OG detergent, p14-liposomes were subjected to SM2 Bio beads during dialysis at 4°C (Rigaud et al., 1988). To control for the addition of the detergent, standard liposomes were also subjected to addition of OG

and dialysis even though no protein was inserted. FITC was added to the thin film during hydration as this is the simplest method of encapsulating hydrophilic cargo within the liposome core. To measure the size of the liposomes after protein insertion, dynamic light scattering (DLS) was performed. DLS analysis revealed the size of the liposomes with or without the insertion of protein was comparable of 158.9 $\pm$ 1.7 for standard and 152.1 $\pm$ 1.1 for p14 liposomes (Table 3.2).

Table 3.1 Lipid Profile for Assembly of p14 Liposomes

Lipid	Desired molar ratio (%)	Molecular Weight (g/mol)	Volume of Buffer (per flask) (ml)	Concentration of each lipid solution (mg.ml)	Desired final lipid concentration (liposomes) (mM)	Amount of lipid solution required (µl)
DOPC	60	786.13	1	25	20	377
DOPE	30	744.05	1	25	20	179
Chol	4	386.66	1	25	20	12
DC-Chol	6	501	1	25	20	24
Total %	100	%			Total	580

Table 3.2 Particle Size Analysis using Dynamic Light Scattering (DLS)

Liposome Group	Diameter (nm)
Standard	158.9 $\pm$ 1.7
P14	152.1 $\pm$ 1.1

P14 liposomes increase intracellular FITC delivery in PC3 cells

Liposomal uptake studies were performed on PC3 cells, to test the efficiency of the p14 FITC delivery. Standard (no protein) and fusogenic (p14) liposomes were prepared and incubated on the cells for 1hr at 4°C. The liposome preparations were incubated on the cells at 4°C to inhibit endocytosis ensuring the FITC internalization was dependent on the p14 fusion ability (Meulendyke et al., 2005). Liposomes were then washed off and cells were returned to 37°C to allow internalization (Leser et al., 1996). Immunofluorescence microscopy images (Figure 3.2A) displays a greater green fluorescence signal in the cytoplasm of the cells incubated with the p14-liposomes. In contrast, there was a decrease in cellular fluorescence when cells were incubated with std liposomes. To quantify the green fluorescent signal in the cytoplasm of the PC3 cells we measured using flow cytometry. PC3 cells incubated with p14-liposomes significantly increase the intracellular delivery of FITC ($p<0.05$) (Figure 3.2B). These uptake studies verify the novel mechanism of p14 liposomes and their ability to increase intracellular delivery independent of endocytosis. We repeated the same experiment on two different cell lines, breast cancer (MDA-MB231) and human fibroscarcoma (HT1080) cells to ensure p14 liposomes increase intracellular delivery on a variety of cancer cells. Appendix B demonstrates p14 liposomes increase intracellular delivery to three different human cancer cells. Once confirming the fusogenic potential of p14, we developed a fusogenic targeted fusion protein (p14-bombesin) to bind to prostate cancer cells via the GRPR.

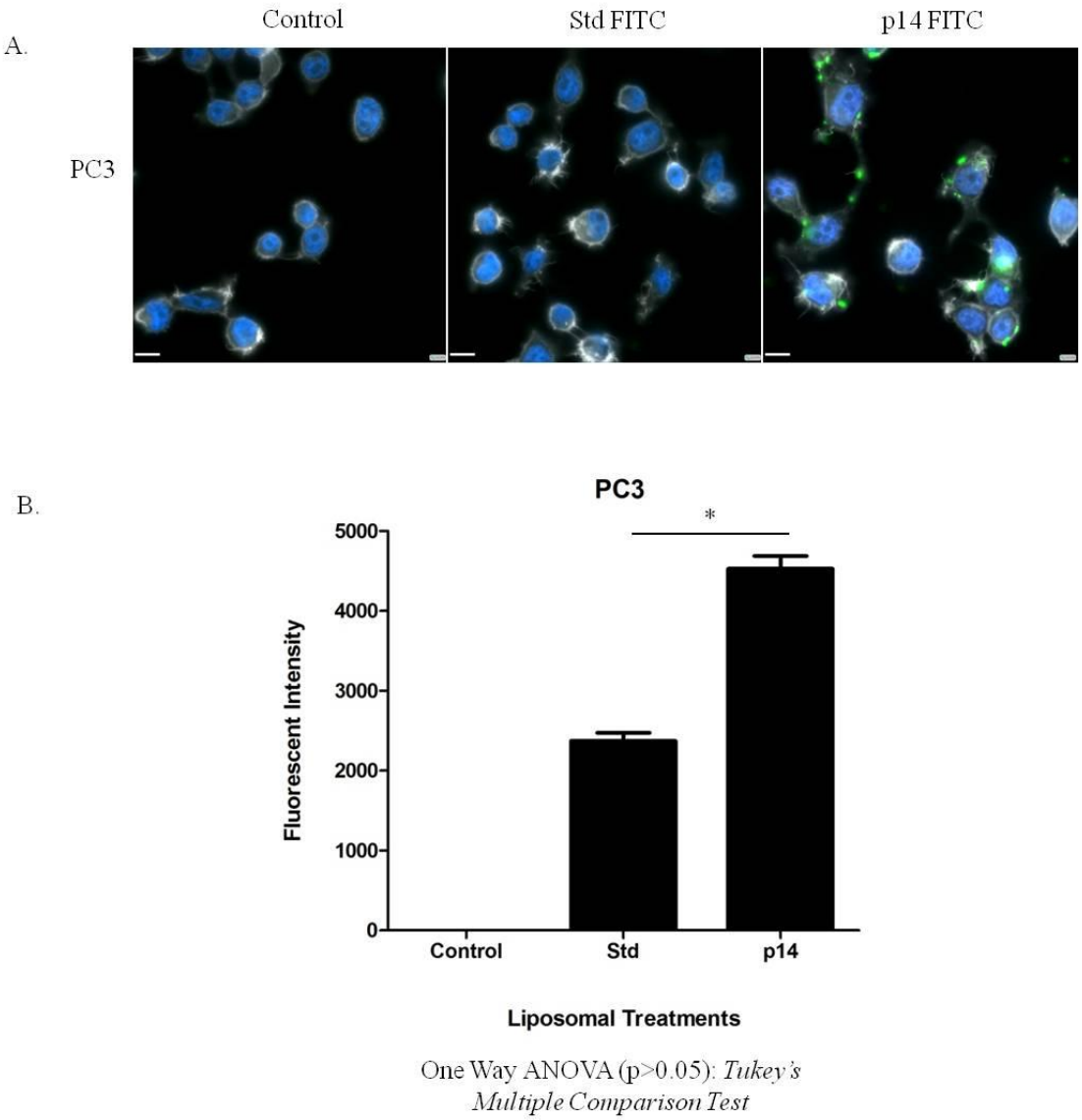

Figure 3.2 p14-liposomes deliver significantly more FITC to the cytoplasm of PC3 cells compared to standard liposomes.
Liposome uptake analysis of FITC, delivered by standard (Std) liposomes (no protein) and fusogenic liposomes (p14 protein). Representative fluorescent images of one field of view of PC3 cells at 20 X magnification. The cells were stained with a nuclear stain (DAPI, blue) and an actin filament stain (phalloidin). The green fluorescent signal represents the intracellular FITC uptake. B) Quantification of the fluorescence intensity cells using Flow Cytometry. Fluorescent intensity $\pm$ standard error of the mean (SEM) is shown for the treatments and this data is representative of n=10 experiment. One way ANOVA ($P<0.05$) *Tukey's Multiple Comparison Test*.

3.2 Objective 2: The creation of the p14-Bombesin peptide and the Evaluation of the Functionality

Can a targeting ligand be attached to the C-terminus of the p14 protein to serve as a targeting molecule for prostate cancer without disrupting the fusogenic capability of the p14 protein?

Following confirmation that p14 increases intracellular delivery, we tested if the C-terminus will tolerate a targeting peptide. By creating multifunctional liposomes we could increase intracellular delivery and specificity for prostate cancer.

Using PCR amplification, successful conjugation of bombesin to the C-terminus of p14 creates a targeted fusogenic construct

It has been demonstrated that the C-terminus of the p14 protein can tolerate modifications without disrupting the N-terminal fusogenic domain (Corcoran & Duncan, 2004; Corcoran et al., 2004). We hypothesized that conjugation of a targeting peptide to the C-terminus of the p14 protein would create a novel targeted fusogenic protein. We choose bombesin as the targeting peptide because previous studies in our laboratory have demonstrated the targeting ability of bombesin to the gastrin releasing peptide receptor (GRPR) on prostate cancer cells (Steinmetz et al., 2011). We generated a p14-bombesin fusion protein using polymerase chain reaction (PCR) amplification strategy represented in a schematic in Figure 3.3A**.** Our strategy involved designing a reverse primer containing the entire bombesin sequence. To confirm the PCR fusion of bombesin to p14, a restriction digest was performed using Bam H1 and Xho1 restriction enzymes (RE). The bands present in the agarose gel correlate with the respected DNA size of the

pFastbac vector (4.7 kbp) and the p14-bombesin sequence (465 bp) (Figure 3.3B). The DNA fragments were confirmed by sequencing at Robarts Research (Appendix C).

Expression of p14-Bombesin induces syncytia formation similar to native p14

Once we confirmed the p14-bombesin sequence, we tested the ability to induce multinucleated syncytium formation similar to the assay we used to test the functionality of native p14 in Objective 1. As an initial step to examine the correlation between the rate and extent of syncytium formation, we analyzed the differences between the native p14 and the newly created p14-bombesin. Quail fibroblast (QM5) cells were transfected with the original pFastBac-p14 vector (positive control) and the pFastBac-p14-Bombesin. Visualized using fluorescent microscopy the cells were stained with CellTracker green to identify the multinucleated cell bodies. Both the p14 and p14-bombesin induced formation of small syncytia at 6hr post-transfection which increased to larger countable syncytia by 8hr (Figure 3.4). In summary, the addition of the bombesin sequence to the C-terminus of p14 did not disrupt the ability to form enlarged multi-nucleated cells.

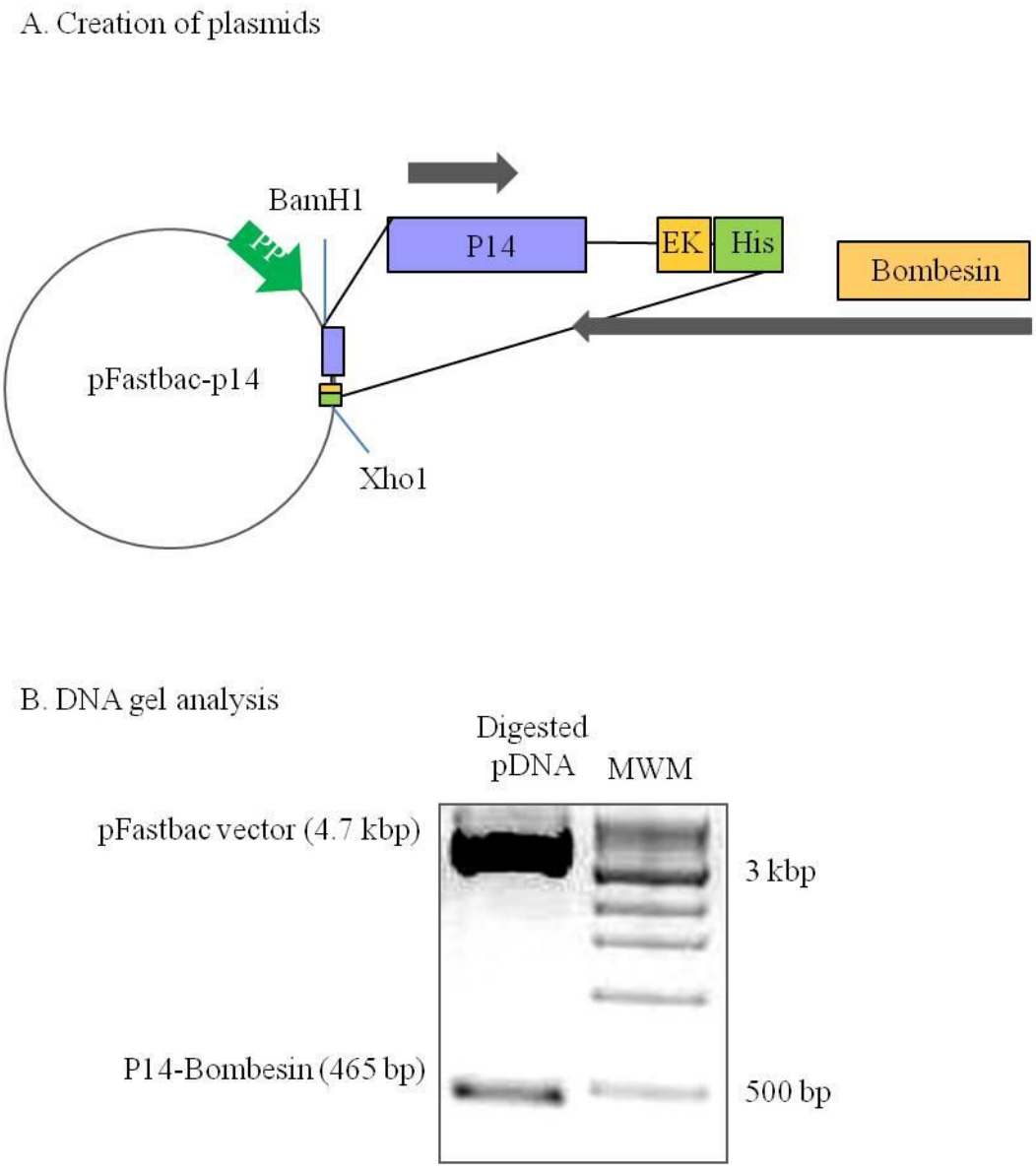

Figure 3.3 Construction of the p14-Bombesin Fusion protein.
A) Schematic of the creation of the pFastBac-p14-bombesin. Bombesin was cloned into the pFastbac-p14 vector between BamH1 and Xho1 by designing a reverse primer that contained the entire bombesin sequence for polymerase chain reaction (PCR) amplification. The p14 construct includes two tags: EK enterokinase cleavage site and Histidine 6x (his).
B) PCR analysis of p14-bombesin was verified by digesting pFastBac-p14-bombesin using the restriction enzymes (RE) BamH1 and Xho1 and ran on a 0.7% agarose gel in 1x Tris/Borate/EDTA buffer (TBE) buffer. The bands correlate with the digested fragments of pFastBac vector (4.7 kbp) and p14-Bombesin (465 bp). The p14-bombesin sequence was confirmed using DNA sequencing technology.

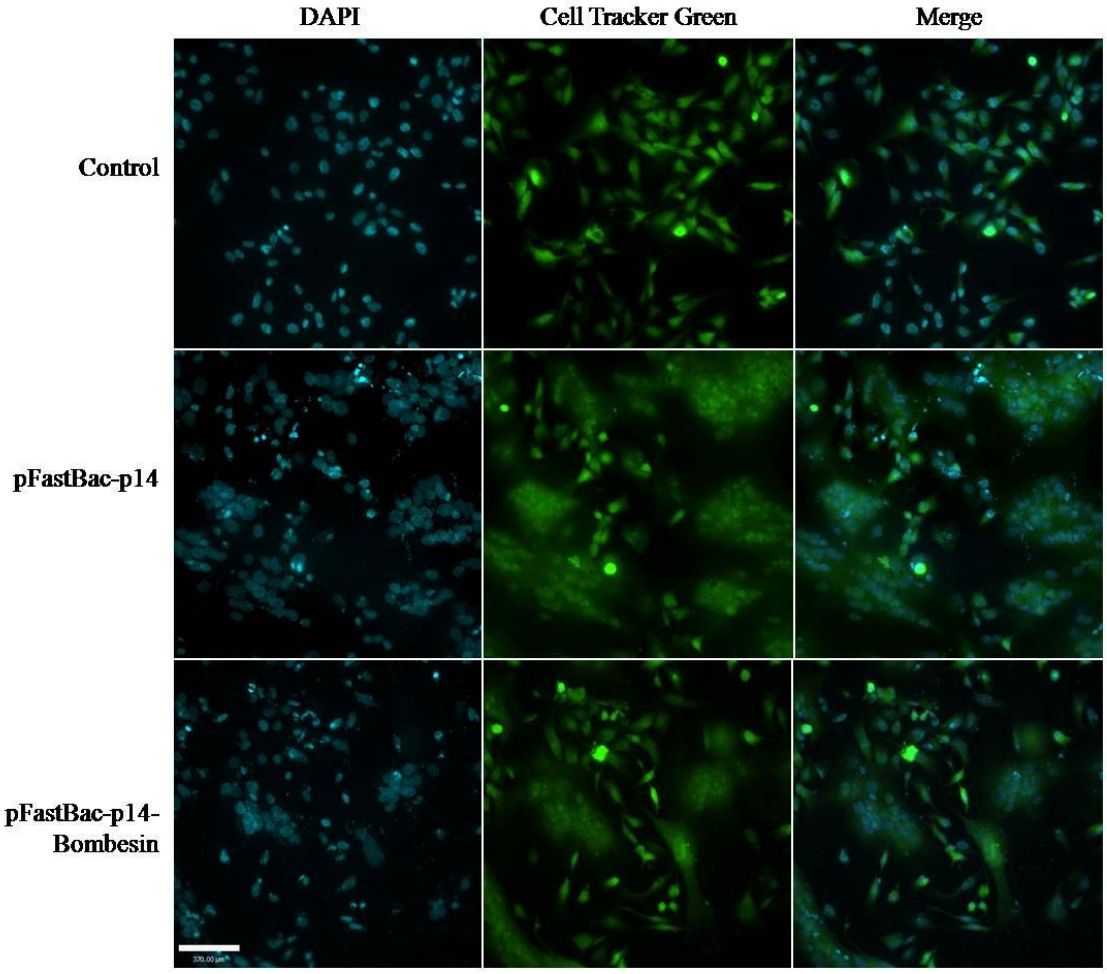

Figure 3.4 Expression of p14-bombesin results in syncytia formation similar to p14.

Epifluorescence imaging of quail muscle (QM5) cells incubated with 1 µg of pFastBac-p14 and pFastBac-p14-bombesin using Lipofectamine 2000. QM5 syncytia were Cell Tracker green stained at 8hr after transfection. Syncytia formation clearly visible in both the p14 and p14-bombesin images.

Calculating the syncytia index using flow cytometry approach

To determine whether the extent of syncytium formation was greater in pFastBac-p14-bombesin expression, we developed a high through-put quantitative analysis to measure the multinucleated cells by flow cytometry. To accommodate the large multinucleated cells, we utilized a large cell Biosorter to perform our flow cytometry experiments and stained the nuclei with Sytox green. To ensure the quantification was accurate, we obtained samples of single events after analyzing by flow cytometry. The representative images in Figures 3.5A display the differences between control and syncytia cells that were sorted after the fluorescence was analyzed. The control cells contain one nucleus whereas the syncytia cells contain many nuclei, representative of the green fluorescent nuclei (Figure 3.5A). The flow cytometry quantification establishes no significant difference between the syncytia formation produced by p14 or p14-bombesin expression (Figure 3.5B). Even though there is little to know in regard to how these FAST proteins induce membrane fusion except for the importance of the N-terminal myristoylation site, we now confirm that the modification of the C-terminus of p14 does not alter the rate or extent of the syncytium formation. These results support the finding made by Corcoran et al that deletions of the C-terminus do not disrupt the cell-to-cell fusion (Corcoran & Duncan, 2004). However, our finding differed from their study which found the deletions delayed the rate of syncytia formation, whereas conjugating bombesin to the C-terminus of p14, did not change the rate of formation.

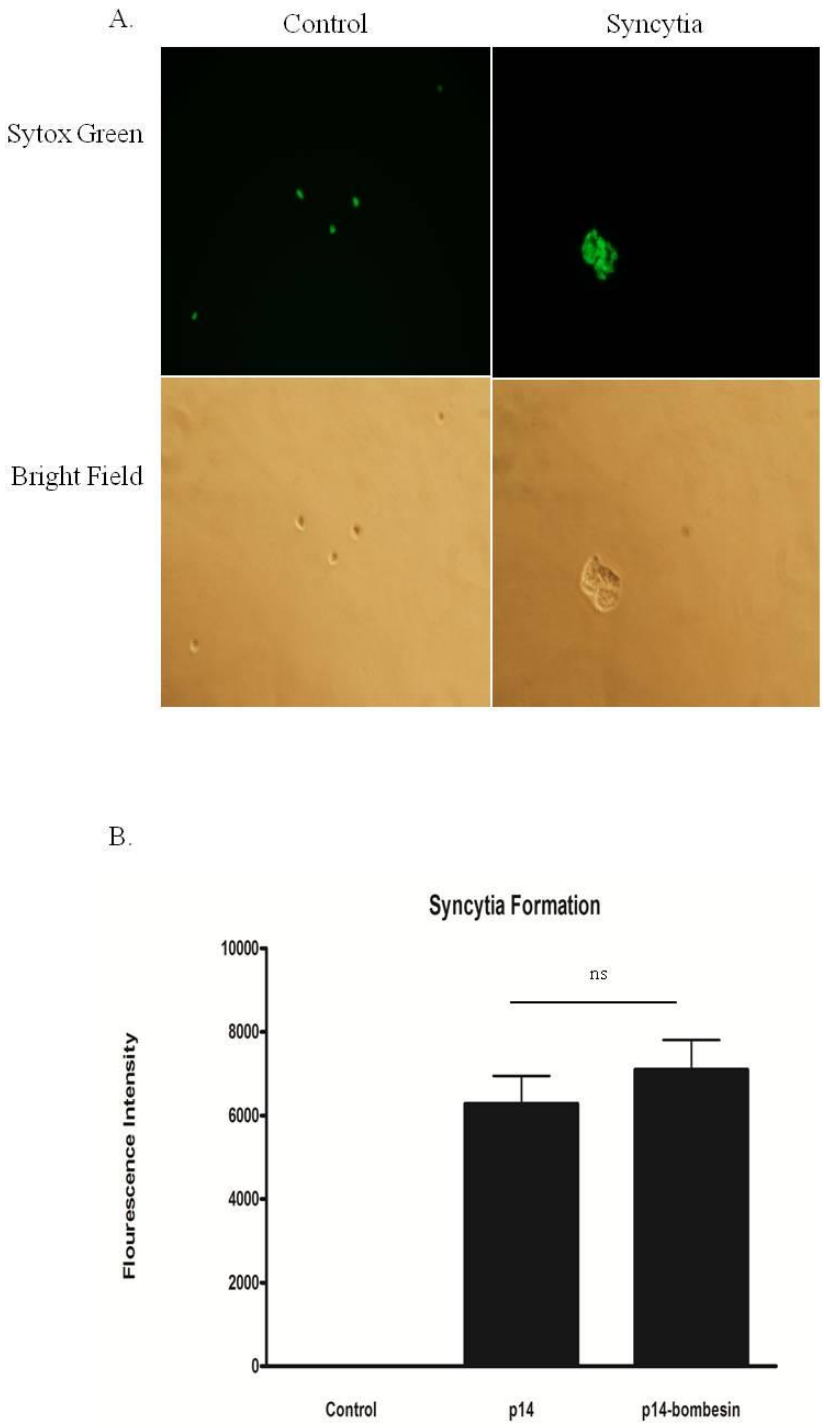

Figure 3.5 Quantification of syncytia formation in QM5 cells using Flow Cytometry.

A) Representative images of the multinucleated cells, the QM5 control cells contained 1 nucleus whereas expression of the p14 and p14-bombesin contained multiple nuclei. B) Quantification of the green fluorescent intensity correlates with the number of nuclei present. Expression of p14 and p14-bombesin were not significantly different for formation of syncytia.

Purification of p14-bombesin fusion protein requires a two step process to extract enough protein

Cobalt resin has a high affinity for his-tag on p14-bombesin protein

The baculovirus expressed p14-bombesin was purified in a two step purification process (Top et al., 2005). The p14-bombesin sequence contains a histidine-tag for purification purposes. Histidine is one of the most prominent affinity tags for protein purification (Ley, et al., 2011). To purify p14-bombesin, the crude cell lysate was first incubated with the Talon™ cobalt resin for 3hr at 4^{o} C for initial purification to ensure total binding of the p14-bombesin-histidine tag. Cobalt has a high binding affinity to histidine and consequently binds to the p14-bombesin protein and other histidine rich proteins from the crude sample (Gaberc-Porekar & Menart, 2001). The resin was washed with extraction buffer twice to remove unbound protein and the p14-bombesin was eluted from the resin with imidazole containing elution buffer. Imidazole is used to displace the His-tagged p14 protein, freeing the p14 protein. The extraction of the p14-bombesin protein using the Talon™ resin was identified by coomassie stain (Figure 3.6A). To ensure the process extracted the p14-bombesin we loaded the extraction from the Talon compared to the wash steps to ensure that we extracted all the p14-bombesin (Figure 3.6A).

Ion Exchange Chromatography further purifies p14-bombesin protein for a homogenous population

To further recover the p14-bombesin protein we use a second purification step using an ion exchange column (HiTrap Sepharose High Performance). The ion exchange column

contains a strong cation exchange medium to bind our anionic p14-bombesin protein. The adsorbed p14-bombesin protein is eluted using buffers varying in pH and ionic strength to dislodge the p14-bombesin protein and collect as individual fractions and analyzed separately (Appendix D). We assessed the ion exchange fractions using silver stain analysis and comparing p14-bombesin purified protein to the relative migration of the standard purified p14 protein (Figure 3.6B). In the end, approximately a total of 4 mg of p14-bomesin protein is purified from a large scale protein batch. Despite the quantity of purified protein, only a portion of the fractions were myristoylated and therefore functional.

A. Coomassie stain

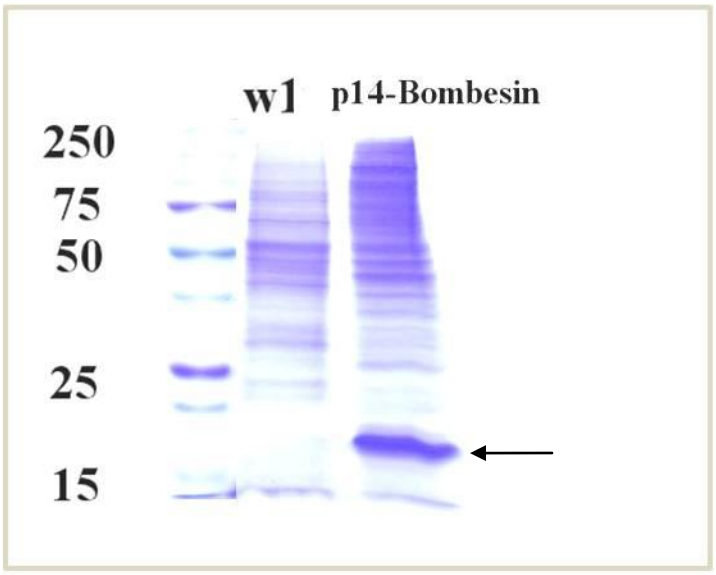

B. Silver Stain

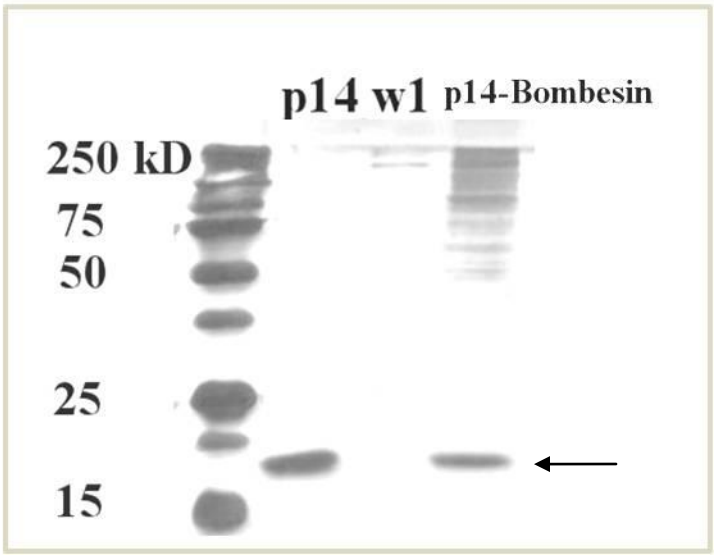

Figure 3.6 Purification of p14-bombesin
Cell lysates of sf21 cells infected with p14-bombesin baculovirus were purified using cobalt Talon® resin and ion exchange chromatography.
A) Proteins present were resolved by SDS-PAGE and detected by Coomassie after cobalt resin. W1 (First wash of the resin) and the arrow indicates the p14-bombesin ~16 kDa.
B) Silver Staining after the ion exchange chromatography. Native p14 protein was used as a standard to indicate the relative migration, W1 (first wash of the column) and the arrow indicates the purified p14-bombesin.

Analysis of purified p14-bombesin using fusion assay revealed conjugation of bombesin to the C-terminus does not disrupt the fusion motif of p14 protein

FAST proteins mediate synctyium formation and we examined the kinetics of syncytium formation of the purified p14-bombesin protein. To test the functionality of the purified p14-bombesin protein, QM5 cells were incubated with p14-bombesin protein delivered with Lipofectamine, followed by fluorescence microscopy. Since expression of the pFastBac-p14-bombesin has been confirmed to mediate cell-cell fusion, we performed a similar assay to evaluate the functionality of the purified p14-bombesin protein. Syncytium formation was assessed by staining the cells with CellTracker Green at 8hr post transfection and visualized using fluorescent microscopy (Figure 3.7). The purified p14-bombesin protein demonstrated significant syncytia formation comparable to the fusion active standard p14, verifying that the p14-bombesin protein is functional. These results revealed that bombesin conjugated to the C-terminus of p14 did not disrupt the ability of p14 to induce cell-to-cell fusion and elucidates that the p14 N-terminus was myristylated. Furthermore, the different protein fractions (Appendix D) were all assayed for fusion activity and the representative images in Figure 3.7 was analysis of the E4 p14-bombesin fraction. Most commonly protein fractions from E3 to E6 are the functional fractions. However, the assay is perfomed on all fractions to ensure what protein fractions are fusion active and therefore myristylated.

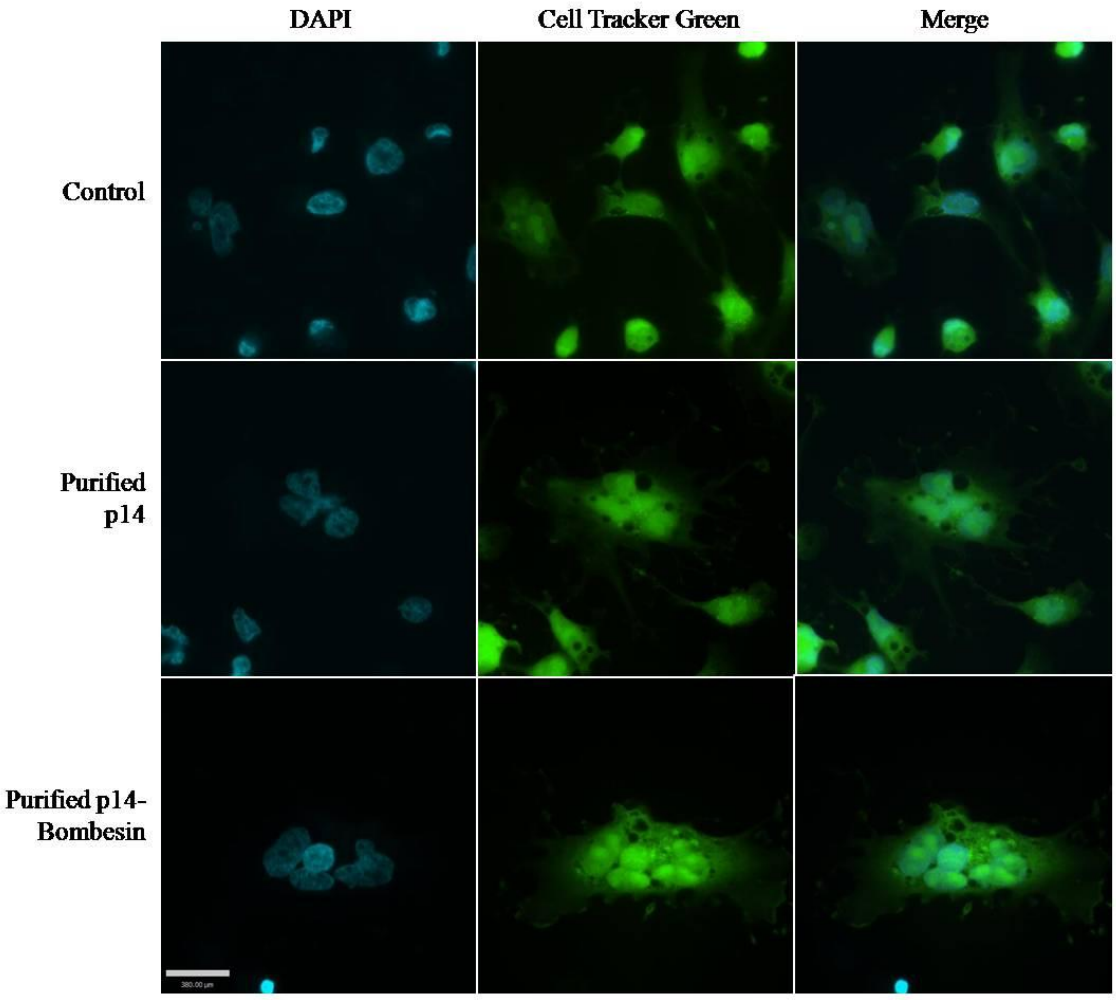

Figure 3.7 Purified p14 and p14-bombesin protein forms multinucleated cells confirming the protein is functional.
Immunofluorescence imaging of QM5 cells incubated with 4 µg of purified p14 or p14-bombesin protein. Proteins were solubilized in Lipofectamine and incubated on QM5 cells for 8hr. Syncytia were visualized by staining the nuclei with DAPI (blue) and the cytoplasm with cell tracker (green) using epifluorescence microscopy. This syncytia assay verifies that the purified p14-bombesin protein is functional comparable to the p14 standard.

3.3 Objective 3: Assembly of Targeted Liposomes and assessment of FITC delivery to Prostate Cancer Cells

Targeted Liposomes Increase uptake of FITC in Prostate Cancer Cells In Vitro

The purpose of this study was to validate our hypothesis that bombesin decorated liposomes allow target recognition to prostate cancer (PC3) cells. The targeted fusogenic liposomes were assembled in the same manner as the p14-liposomes were in section 3.1. For targeted delivery systems to be effective, the target should be up regulated on the cancer cells of interest. Human PC-3 cells are a well studied cell line for gastrin releasing peptide receptor (GRPR) targeting because they express approximately 48000 receptors per cell. To evaluate the targeted fusogenic properties of the p14-bombesin protein-containing liposomes, we encapsulated a fluorescein isothiocyanate (FITC) (1 mg/mL) inside cationic liposomes, standard (no protein), fusogenic (p14 protein) and targeted fusogenic (p14-bombesin protein). We incubated the liposomes on PC3 cells for 1hr at 4^0C and measured the uptake of FITC using confocal microscopy and flow cytometry. Figure 3.8 is representative fluorescent confocal microscopy images of PC3 cells and the green fluorescence (FITC) intensity is indicative of the efficiency of the different treatment groups as the targeted (p14-bombesin) liposomes exhibit a greater distinction in the cytoplasm of the PC3 cells. Untargeted liposomal treatments had significantly less FITC accumulation in PC3 cells (Figure 3.8). According to Figure 3.8, targeted liposomes significantly increase the FITC uptake into PC3 cells compared to both standard liposomes (no protein) and fusogenic liposomes (p14) ($P<0.05$).

Furthermore, p14-liposomes also had significantly more FITC compared to standard liposomes, confirming that p14 increases the intracellular delivery.

The flow cytometry results were reflected in the fluorescence images captured by the confocal microscopy. Flow cytometry histograms are presented in Figure 3.9A and the quantification in Figure 3.9B reveals the FITC expression is very consistent with the fluorescent microscopy images. In summary the GRPR are an attractive target for the navigation of therapeutics because the receptors are widely expressed on the surface of prostatic cancers. Moreover, these results establish that the addition of bombesin peptide to p14-liposomes enables successful targeting of PC3 cells increasing the intracellular delivery beyond that of the fusogenic liposomes.

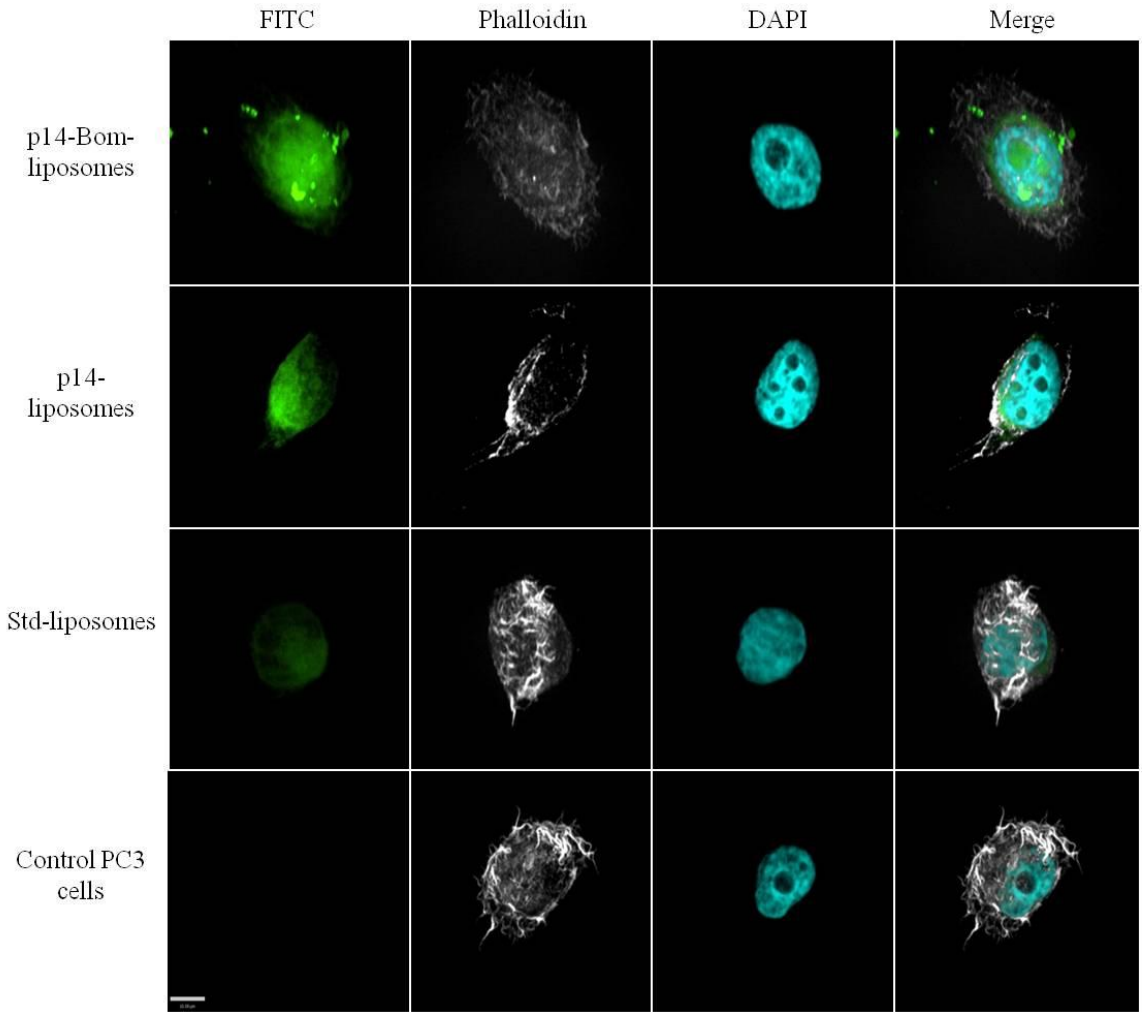

Figure 3.8 p14-bombesin liposomes increase the intracellular delivery of FITC to PC3 cells.
Fluorescence confocal microscopy images of p14-bombesin, p14, or standard liposomes encapsulating FITC incubated with PC-3 prostate cancer cells. Nucleus (DAPI stain) and actin filaments (phalloidin stain). These images were taken at 63 x magnification with an oil surface.

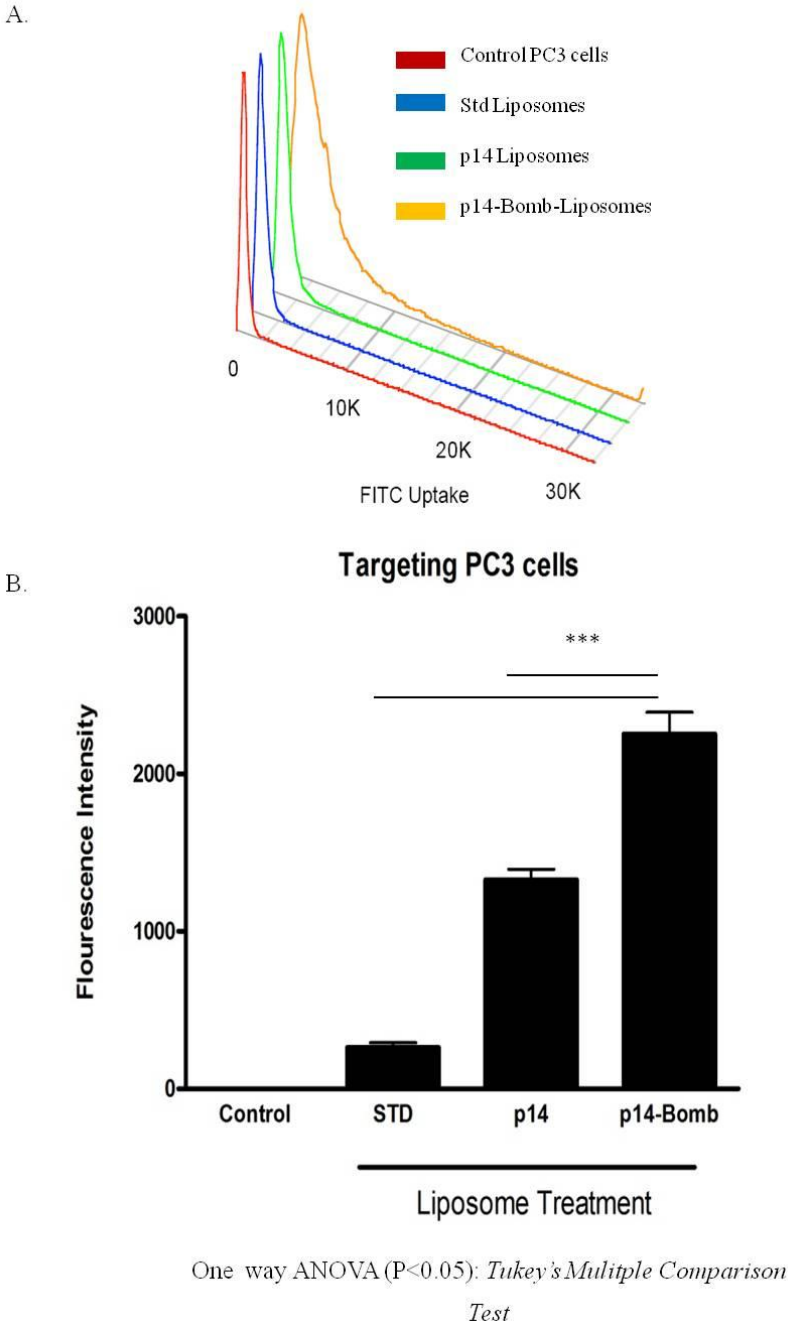

Figure 3.9 p14-Bombesin Liposomes Significantly Increase FITC in PC3 cells
A) Histogram of FITC signal using flow cytometry of PC3 cells incubated with liposomes. B) Quantification of uptake of liposomes into PC3 cells using flow cytometry. Mean percentage of the green fluorescent positive cells ±standard error of the mean (SEM) is shown for each treatment. P14-bombesin is take up more efficiently than p14-liposomes ($p<0.05$). This flow cytometry data is representative of n=8 experiment with at least 10000 events collected. One way ANOVA ($P<0.05$): *Tukey's Multiple Comparison Test.*

P14-Liposomes are internalized within PC3 cells and not bound to the cell surface

The previous study we studied the binding and uptake of the p14-bombesin liposomes to PC3 cells by measuring the fluorescence of the cell with flow cytometry. However, this method does not definitely distinguish between the liposomes bound to the surface or intracellularly. Using confocal microscopy and imaging using 3D stacks, we were able to distinguish the localization of the FITC in PC3 cells following p14-bombesin liposomal treatment. The 3D representative images in Figure 3.10 demonstrate the presence of the FITC (green fluorescence) located between the actin filaments of the cell membrane (orange fluorescence) confirming the internalization of the FITC. Attachment of the bombesin peptide did not alter the p14 ability to induce liposomes to cell fusion allowing direct cargo delivery to the cytoplasm of the cells.

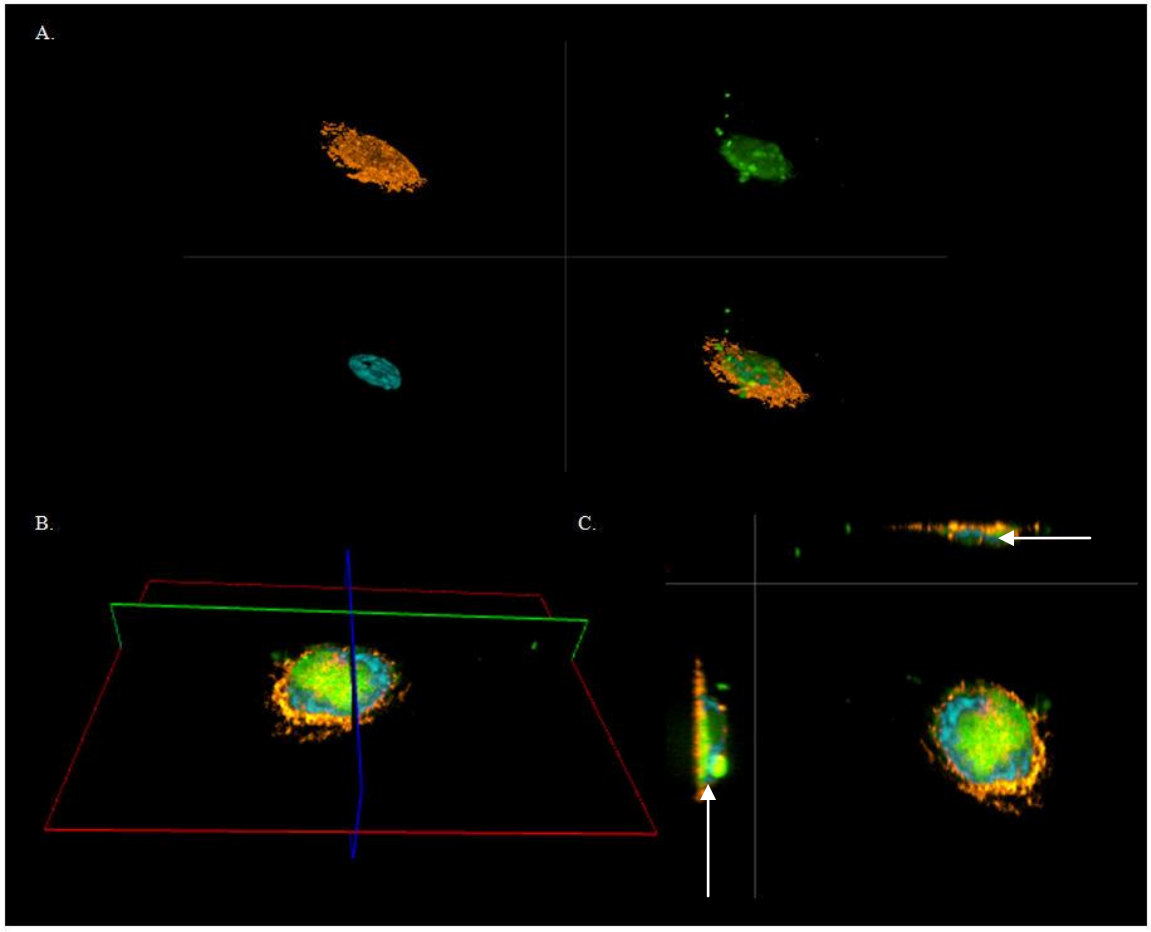

Figure 3.10 p14-Bombesin Liposomes Deliver FITC Intracellularly into Prostate Cancer Cells (PC3 cells).
Fluorescence confocal microscopy 3-dimensional images of p14-bombesin liposomes incubated on PC3 cells. A) Separate channels; green (FITC), orange (actin filaments of the cytoplasm), blue (nuclear stain) B) the orientation of the cross-section C) Cross-section (confocal z stack) demonstrating the intracellular FITC signal.

3.4 Objective 4: Evaluation of the Specificity of Bombesin Targeted Liposomes

Testing the uptake of Targeted Liposomes on Benign Prostatic Hyperplasia cells

After we established p14-bombesin liposomes significantly increased the FITC uptake in PC3 cells, we determined if this targeting is explicit for cells with a high density of GRPR. To verify the expression of GRPR we used Western blot analysis in different prostate cells, human prostate cancer cell line (PC3) and a non-cancerous benign prostatic hyperplasia (BPH) cell (Figure 3.11A). Bands of tubulin were used as a loading control for the normalization of the GRPR bands. PC3 cells demonstrated a higher expression of the GRPR compared to the BPH cells, verifying that the PC3 cells were an adequate cell line to test the targeting potential of the p14-bombesin liposomes. Since BPH cells have a lower GRPR protein expression (Figure 3.11A); we used these cells to perform the same experiment as we did on the PC3 cells which over expressed the receptor. The uptake of FITC liposomes in BPH cells, with no protein, p14, or p14-bombesin was evaluated by flow cytometry (Figure 3.11B). Compared to the analysis in PC3 cells, the uptake in BPH cells differed only in the p14-bombesin treatment. There was a significant decrease in FITC uptake of the p14-bombesin liposomes in contrast to the p14 liposomes ($p<0.05$). This is due to the lower GRPR expression in the BPH cells and therefore the p14-bombesin liposomes did not bind to the BPH cells at the same efficiency as they did on PC3 cells which exhibited a higher receptor density. Furthermore, the standard and p14 liposomes had similar FITC uptake comparable to PC3 cells. This is the first evidence

that supports the hypothesis that p14-bombesin liposomes show an increased avidity for GRPR expressing PC3 cells.

A.

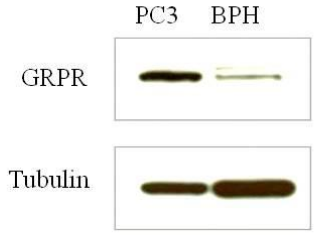

B.

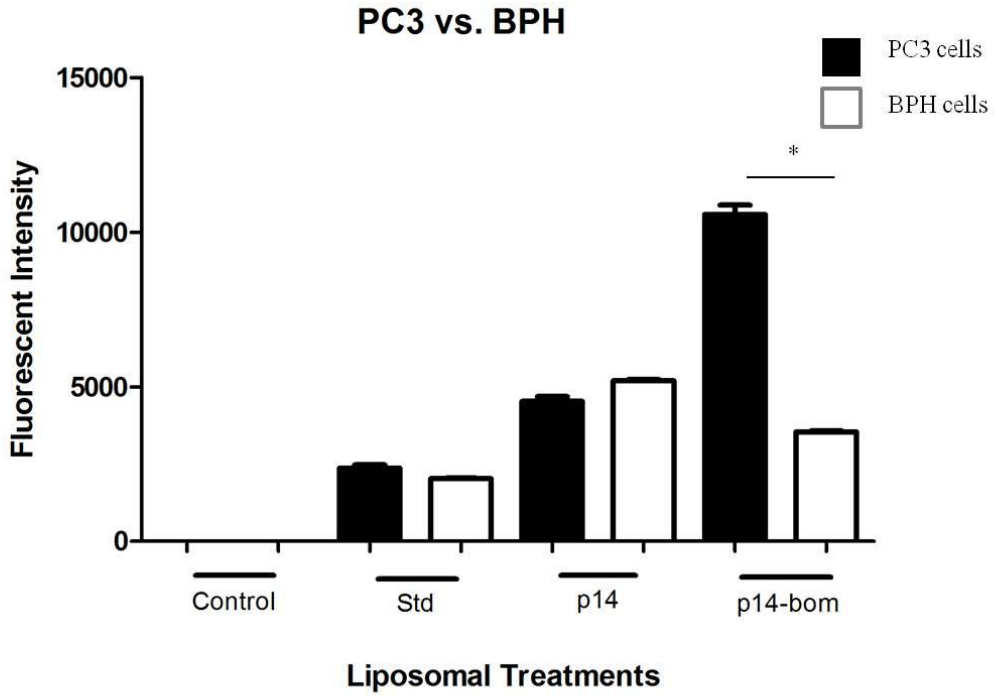

One Way ANOVA ($p<0.05$): *Tukey's Multiple Comparison Test*

Figure 3.11 p14-Bombesin Liposomes Did Not Target Benign Prostatic Hyperplasia Cells

A) Western blot analysis of the protein expression of the gastrin releasing peptide receptor (GRPR) in prostate cancer cells (PC3) and the benign hyperplasia cells (BPH) and tubulin was used a loading control.

B) Quantification of uptake of the liposomes into PC3 cells using flow cytometry. Mean fluorescent intensity $\pm$ standard error of the mean (SEM) is shown for each treatment. P14-bombesin liposomes are taken up less efficiently in BPH cells which have a lower protein expression of the receptor, than PC3 cells. This flow cytometry data is representative of n=5 experiment with at least 10,000 events collected. One way ANOVA ($P<0.05$): *Tukey's Multiple Comparison Test.*

Receptor blocking decreased liposomes decorated with bombesin to PC3 cells

To dissect the targeting ability, in more detail, we performed a receptor block analysis. We have previously reported the bombesin peptide manufactured by the Luyt lab is specific for the GRPR (Steinmetz, et al., 2011). To ensure that the ligand was mediating the binding of the peptide functionalized fusogenic liposomes to prostate cancer cells, PC3 cells were incubated with an excess of free bombesin peptide for 10 min prior to incubation with the liposomes. Flow cytometry analysis resulted in a significant decrease in uptake of the p14-bombesin liposomes in PC3 cells ($P<0.05$) (Figure 3.12). In addition, adding the free bombesin peptide to cells incubated with standard and p14 liposomes did not change the uptake of FITC. The flow cytometry results indicate free bombesin peptide effectively blocks the functionalized fusogenic liposomes from binding to the GRPR in PC3 cells, supporting the hypothesis that p14-bombesin liposomes specifically target prostate cancer cells.

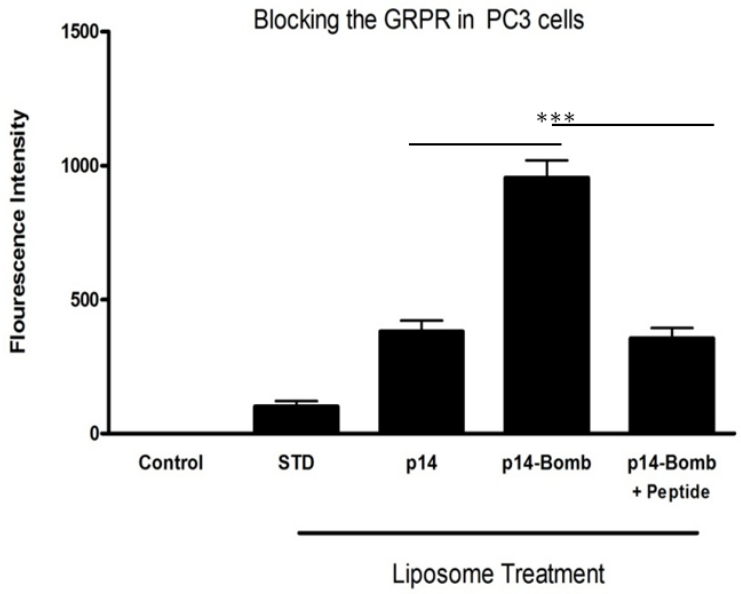

One way ANOVA ($P<0.05$): *Tukey's Mulitple Comparison Test*

Figure 3.12 Receptor Blocking

Quantification of uptake of liposomal FITC into PC3 cells using flow cytometry. P14-bombesin liposomes were effectively blocked by an excess of free bombesin peptide, however the free bombesin peptide did not change the uptake in the other treatment groups (Std and p14). This flow cytometry data is representative of n=2 experiments with at least 10 000 events collected, FITC positive cells $\pm$ standard error of the mean (SEM) is shown for each treatment.

Knockdown of the GRPR Decreased Liposomes conjugated with Bombesin to PC3 cells

Furthermore, to display the preferential association for GRPR expressing cells, we evaluated the uptake of p14-bombesin liposomes on PC3 cells with a lower GRPR expression. We used small interfering RNA (siRNA) technology to knockdown the GRPR in PC3 cells. Transfecting 20 nM GRPR siRNA we decreased the GRPR expression in PC3 cells. Although the transfection only resulted in partial knockdown, validated by Western blot analysis (Figure 3.13A), we can significantly decrease the FITC uptake of p14-bombesin liposomes compared to uptake in normal PC3 cells (Figure 3.13B). Due to the inability to completely knockdown the receptor, the FITC uptake of p14-bombesin liposomes in siRNA transfected PC3 cells remained significantly higher than the uptake of p14 liposomes. Despite this result, the findings demonstrate a decrease in uptake once the GRPR protein expression was lowered. Together, these results confirm liposomes targeted with bombesin peptide showed a significant preference to associate with PC3 target cells over PC3 cells with a lower GRPR expression.

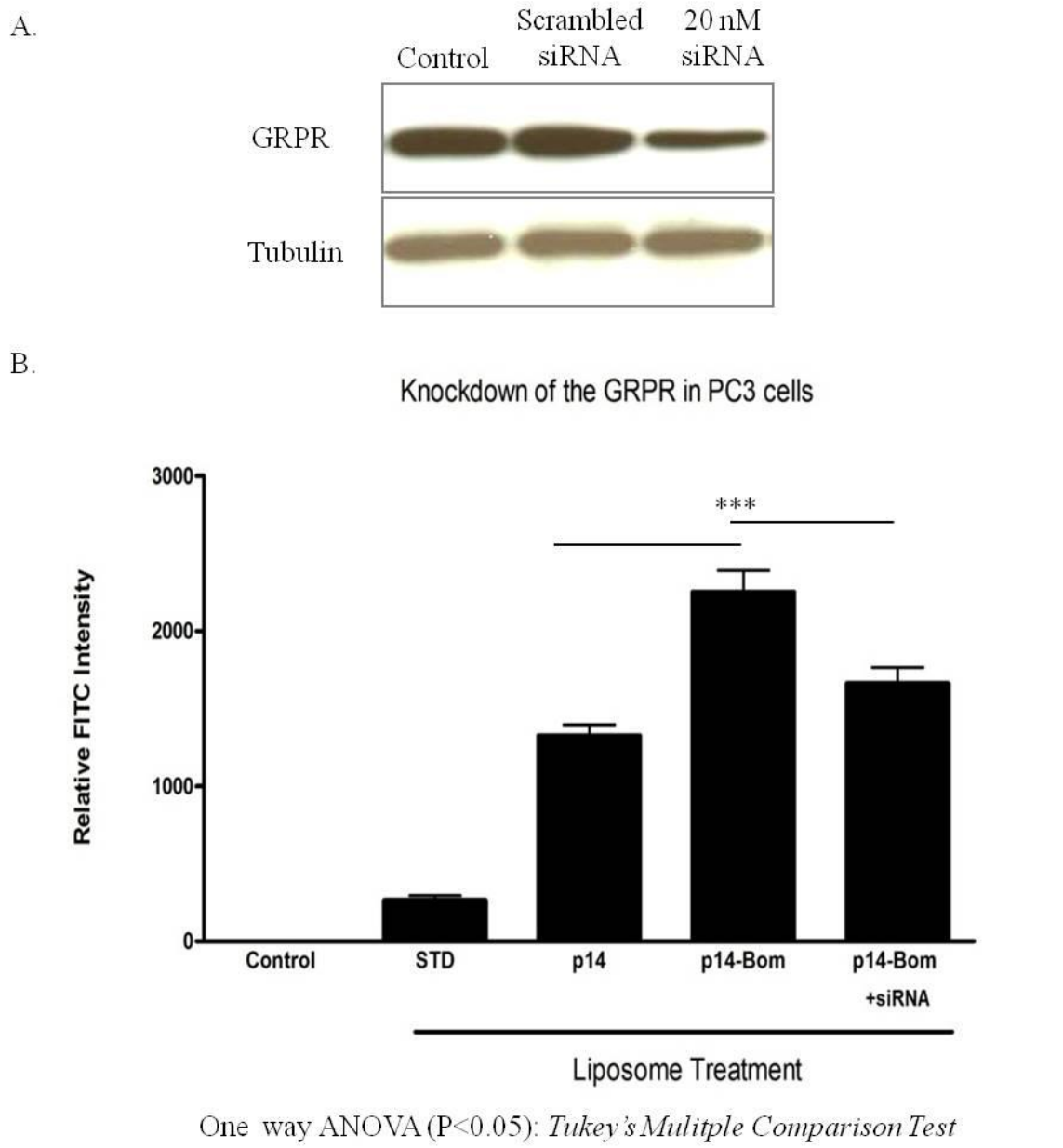

Figure 3.13 Knockdown of GRPR in Prostate Cancer cells Decreases p14-Bombesin uptake

A) Western blot analysis of the protein expression of the gastrin releasing peptide receptor (GRPR) in prostate cancer cells (PC3) and tubulin was used as a loading control. PC3 cells transfected with a negative siRNA and 20 nM of GRPR siRNA.
B) Quantification of uptake of the liposomes into PC3 cells using flow cytometry. Knockdown of the GRPR, using 20 nM siRNA effectively decreased the uptake of the p14-bombesin liposomes. This flow cytometry data is representative of n=3 experiment with at least 10 000 events collected and FITC positive cells $\pm$ standard error of the mean (SEM) is shown for each treatment. One way ANOVA ($P<0.05$): *Tukey's Multiple Comparison Test*.

3.5 Objective 5: Evaluate the Intracellular Delivery of Nucleic Acids

WS improves Encapsulation of Nucleic Acids

In this study, we used a previously described "wrapsome" (WS), designed with a core composed of a cationic lipid bilayer DOTAP (1, 2-dioleoyl-3-trimethylammonium-propane) and pcDNA 3.1-GFP plasmid enveloped in the identical lipid bilayer used in the above experiments (Table 3.1). WS efficiently packages the nucleic acid without exposing the negatively charged DNA on the outer surface (Yamauchi, Kusano, Saito, Iwata, Nakakura, Kato, Uochi et al., 2006). We predicted that the addition of the DOTAP core would encapsulate more DNA than the lipid formulation we used in previous experiments. In spite of this, we were apprehensive how the p14 protein insertion process (detergent depletion) would affect these novel wrapped liposomes or if the WS would change the OG %. We determined that the inner DOTAP core had no obvious differences then liposomes without DOTAP, as we used a 0.9% OG for insertion. At the start of the preparation, 100 µg of DNA (measured by a spectrometer) diluted in 1X PBS was added to the dried 5.6 mM DOTAP film. The DOTAP concentration was determined by using a calculation employed to have an equal charge ratio of DNA: DOTAP. Thus, the concentration of DOTAP changes with differing amounts of DNA (Appendix E).

DNA Quantification with Heparin

In previous research, the stability of DOTAP-DNA complexes inhibits the interaction of DNA binding or intercalating agents (Moret et al., 2001). Ethidium bromide (EtBr) and Picogreen are fluorescent probes commonly employed to quantify DNA by measuring the fluorescence intensity. However, these probes are unable to bind to DNA when complexed with DOTAP. In order to release the DNA from DOTAP, polyanionic heparin was assayed. When heparin was added in a final concentration of 12.5µg/µl (determined from Appendix F) both the EtBr and Picogreen could bind to the DNA. Agarose gel electrophoresis demonstrated that DNA was released from DOTAP in the presence of heparin. When DNA was mixed with DOTAP the release was 100% whereas the release of the DNA encapsulated within the DOTAP core was slightly lower which suggests an incomplete release of DNA from the DOTAP (Figure 3.14A).

Picogreen was used to confirm the above results. Similar fluorescence intensities obtained with free DNA and free DNA mixed with DOTAP (Figure 3.14B). In the process of generating DNA encapsulated within DOTAP, we achieved ~75% DNA incorporation, similar to the results above (Figure 3.14). In summary, the DNA was efficiently encapsulated suggesting that a charge interaction between the negatively charged DNA and positively charged DOTAP assisted the efficiency in loading. Moreover, the addition of heparin assisted in the release of DNA from DOTAP to assess an approximate amount of DNA encapsulated, however not an exact determination (Appendix G).

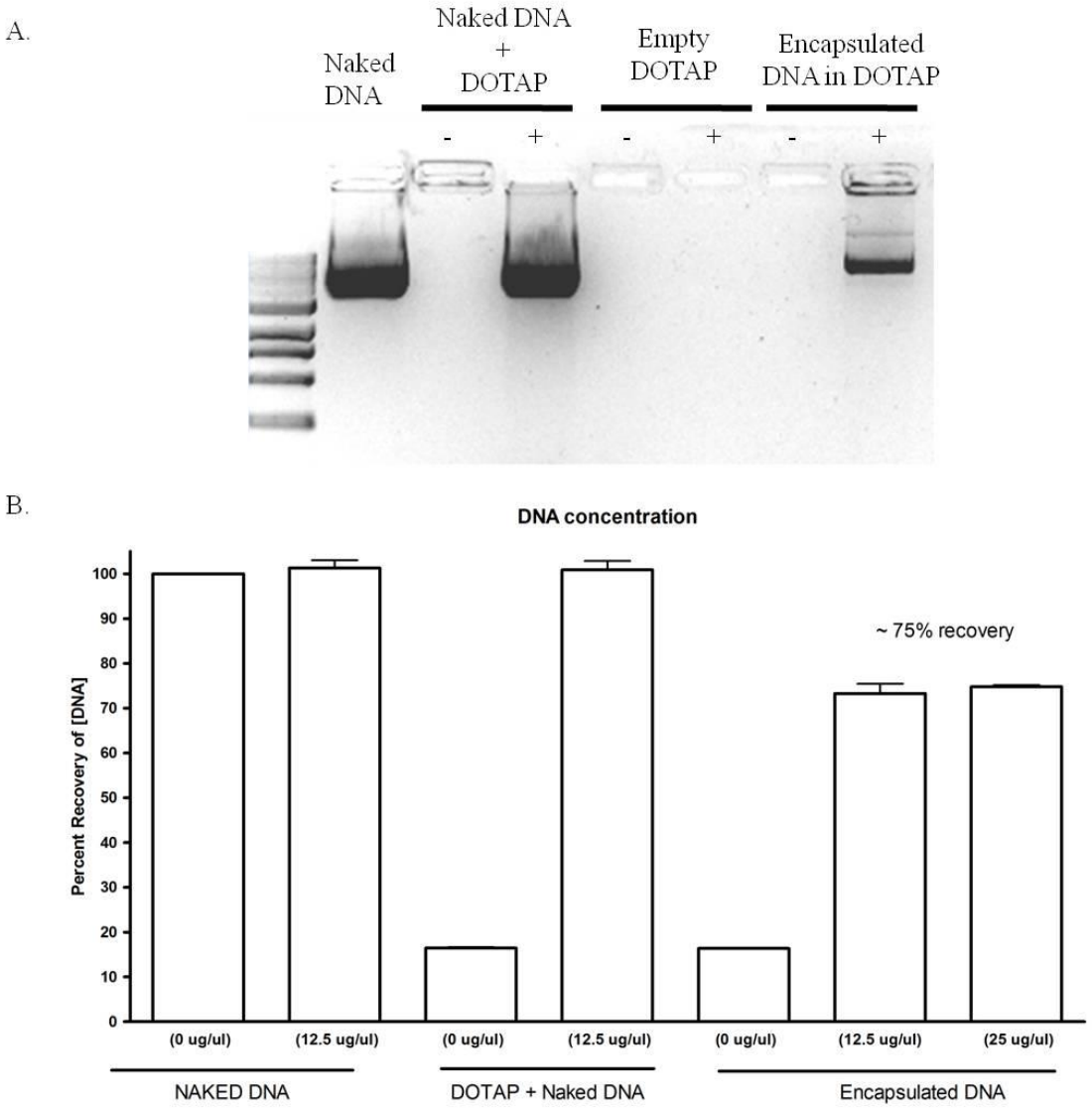

Figure 3.14 Heparin releases DNA from the DOTAP

A) Influence of DOTAP on DNA migration in a 0.7% agarose gel containing Ethidium Bromide (Et Br). The free/ naked pCDNA 3.1 GFP migrated normally. Lanes 2&3, pCDNA 3.1 GFP incubated with DOTAP in the same concentration as the GFP encapsulated within the DOTAP (lanes 6&7). The + indicated the addition of 12.5 µg/µl Heparin for 10 min prior to adding to the gel. Once Heparin was added to both DNA incubated with DOTAP and DNA encapsulated within DOTAP, the bands had migrated and the Et BR was able to bind to the DNA.
B) Quantification of pCDNA 3.1 GFP using Pico Green nucleic acid stain measuring the fluorescent intensity in the presence of heparin (12.5 µg/µl and 25 µg/µl).

Transfection Efficiency of p14-WS

To assess the distribution of DNA delivered by WS within human fibrosarcoma (HT1080) cells, we examined the transfection efficiency of a green fluorescent protein (GFP). Transfections were performed under identical conditions to determine the difference between standard and p14 WS compared to a transfection reagent. We chose Lipofectamine as a positive control as it is a cationic lipid reagent commonly used for *in vitro* DNA transfections. The transfections between p14 and std WS were negligible at 24hr, resulting in green fluorescence comparable of about 1 GFP positive cell/field of view (Figure 3.15). However, at 48hr post transfected p14 observed to have more GFP positive cells (Figure 3.16). As expected, DNA mixed with Lipofectamine had higher transfection efficiency. Previous studies revealed that cationic carriers are quite toxic to cells. However, it is unknown as to what affect other liposome preparations have on the morphology of cells. To test the toxicity of the different liposomal transfection reagents, we did not remove the DNA transfection solutions. Light microscopy was used to determine the outcome of the different liposomal treatments on the cell morphology. Cells exposed to WS were similar in morphology to control cells, whereas healthy looking cells were less apparent following incubation with cationic Lipofetamine (Figure 3.15). In general, cationic lipids increase unfavorable changes in cellular morphology whereas the WS did not subject the cells to toxic effects. Although this study is limited by the lack of statistical data, the preliminary results indicate an efficient method of encapsulating negatively charged nucleic acids and transfection efficiency with lowered toxic effects.

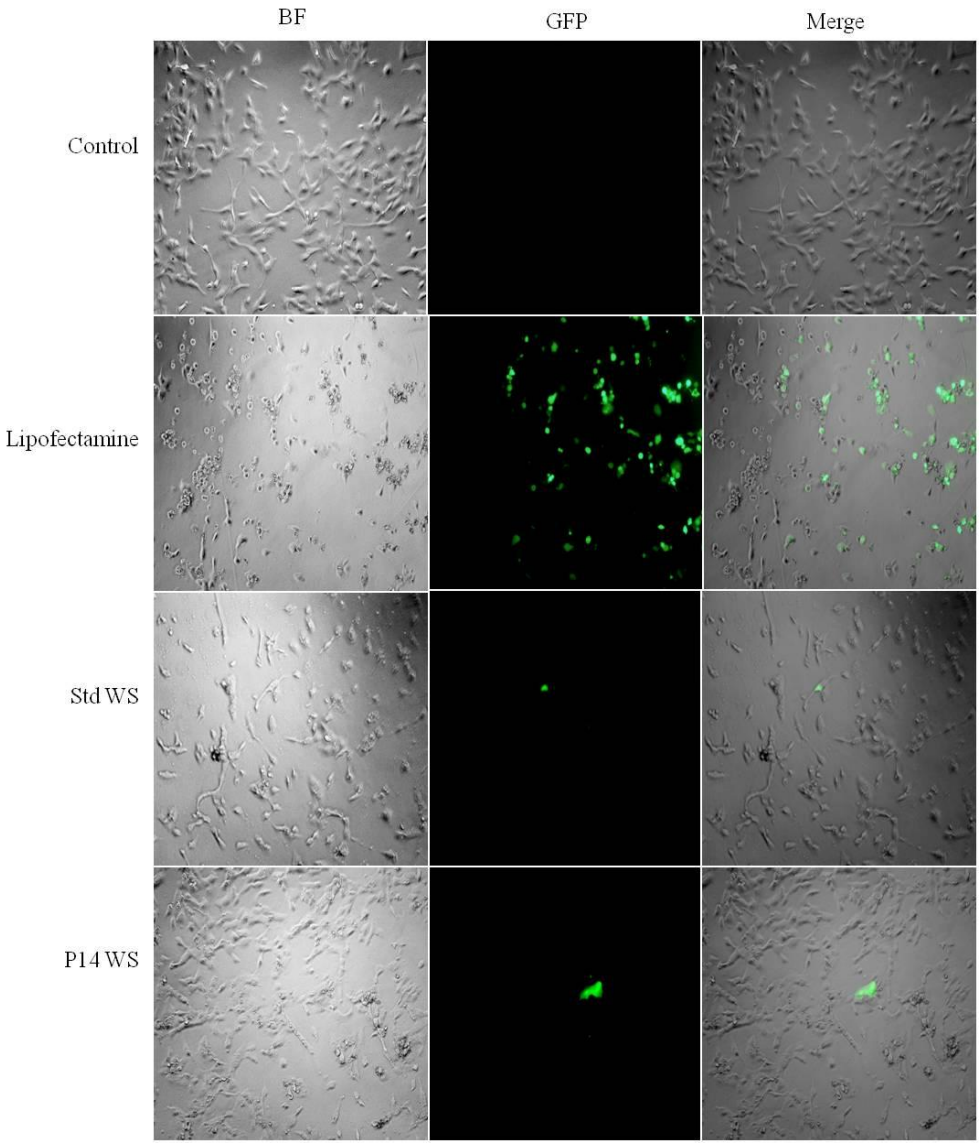

Figure 3.15 24hr GFP Transfection Efficiency

Human fibrosarcoma (HT1080) cells transfected with GFP plasmid by Lipofectamine (positive control), Std WS (no protein), and p14 WS. Control cells were used a negative control. Representative fluorescent microscopy images at 24 hr post-transfection. Transfection reagents were not replaced with fresh medium to visualize the toxicity of the reagents. Lipofectamine reagent clearly changed the morphology of the cells compared to control cells.

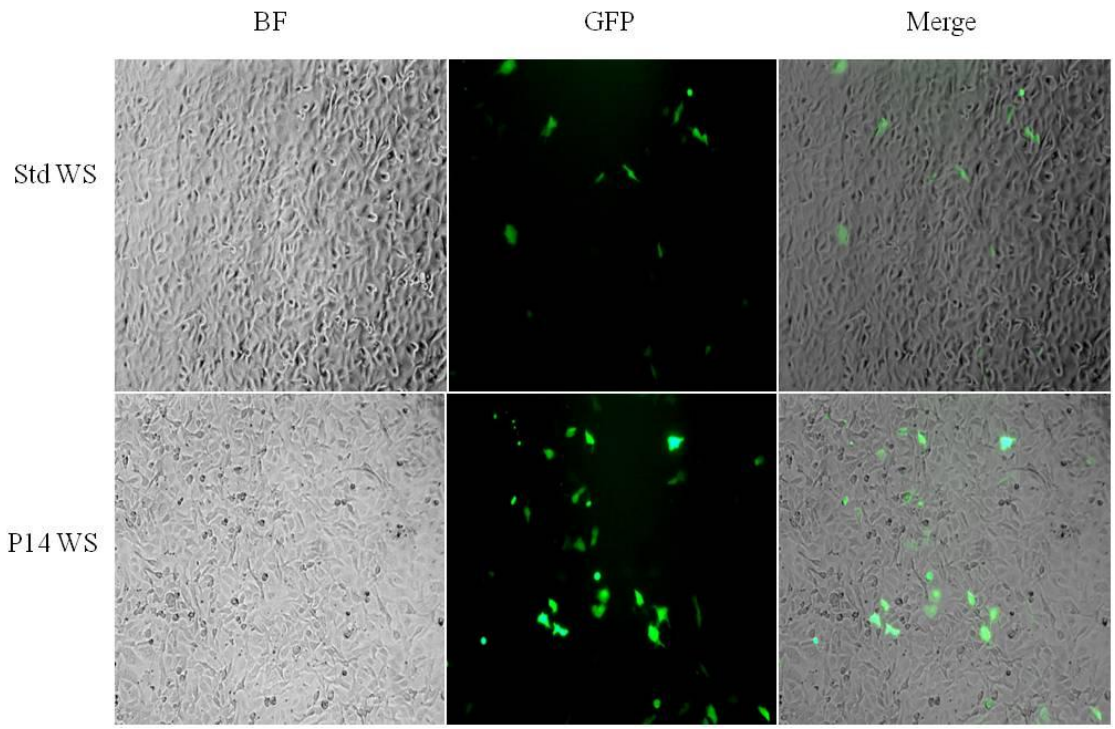

Figure 3.16 48hr Transfection Efficiency of Std and p14 Wrapsomes (WS)

Representative fluorescent microscopy images of human fibrosarcoma (HT1080) cells transfected with GFP plasmid using Std or p14 WS (no protein), and p14 WS at 48hr.

Chapter 4

4 Discussion

4.1 General Discussion and Implications

Prostate cancer remains the most common malignancy in North American men and despite current treatment options, such as radical prostatectomy and active surveillance the therapeutic choices are limited for preserving the quality of life for patients (Bangma, 2011; Canadian Cancer Statistics, 2011). For advanced prostate cancer, chemotherapy is an unfavorable treatment option because the cytotoxicity of available drugs gives rise to unwanted side effects. To counteract this predicament, liposome drug vehicles increase pharmacokinetics and bioavailability by passive targeting through the EPR effect and furthermore, liposomes decrease non-selective toxicity (Matsumura & Maeda, 1986). However, apart from recent advancements, liposomal drug delivery is still inadequate for efficient intracellular delivery. A major obstacle for liposomes is the cell membrane barrier which encumbers the penetration of particles and ultimately impedes the cargo delivery to the cell cytosol. Consequently, the "fusogenic entities" have only overcome this impediment by incorporating different elements which allows the liposomes to escape from the natural endosomal pathway. Endosomal release strategies held great promise to increase cytosolic delivery however the results were sub-optimal (Sakurai et al., 2011; Zhou & Huang, 1994; Zuhorn et al., 2005). Despite decades of research, many liposome formulations do not penetrate the cell membrane and are limited to entry

through endocytosis. The discovery of p14 liposomes is the first to our knowledge a true fusogenic liposome that exhibits fusion capabilities on the cell membrane. A fusogenic liposome carrier would be a beneficial means to deliver therapeutics that could be taken to the clinics. Studies involving the p14 protein reconstituted into liposomes have provided encouraging results *in vitro.* In the present study, we report the validation of a fusogenic protein, p14, which enhances the intracellular delivery bypassing the degradative pathway. The FAST proteins have exceptional structural features and therefore when p14 is reconstituted into an artificial lipid bilayer, the p14 can mediate liposomes to cell fusion. We demonstrated that p14 liposomes increased intracellular FITC compared to standard liposomes on a variety of human cancer cells. This experiment verified that the uptake was independent of endocytosis predominantly due to the fusion motif on p14. This is in accordance with the experiments conducted by Mader et al in which they demonstrated that p14-liposomes increased the LfcinB delivery compared to standard liposomes (Mader et al., 2007). These results concur with the proposed mechanism depicted in Figure 1.1 and provide evidence that p14-liposomes bypass the endocytic pathway by virtue of the fusogenic domain on the N-terminus of P14. Taken together, the fusion activity of p14 verifies the unique feature of this transmembrane protein which increases intracellular delivery but also act as an anchor to attach a targeting peptide.

Prostate cancer targeted nanoparticles conjugated with bombesin have demonstrated both *in vitro* and *in vivo* active targeting results. Previous research in our lab has demonstrated the feasibility of using the small amphibian tetrapeptide to target nanoparticles to human prostate cancer cells *in vitro.* We have also established anti-tumour activity of targeted

particles in an avian embryo model of PC3 cells (Steinmetz et al., 2011). Therefore, active targeting via the bombesin peptide may provide the assistance to overcome hurdles facing therapeutic delivery to prostate cancer. Taken together, we decided to combine the two objectives of research in a single moiety to evaluate the potential of PC3 specific p14-bombesin peptide as a navigating ligand. The justification behind the use of the two unique entities lies in the caveats outlined in the introduction. Liposomes assembled in this study contained a fusogenic domain allowing direct entry into the cell bypassing the endosomal uptake and secondly, liposomes were decorated with bombesin to actively target prostate cancer cells. Furthermore, bombesin did not require chemical conjugation for attachment to the liposomes surface. Instead the transmembrane p14-bombesin protein was inserted directly into the artificial bilayer.

Liposomes functionalized with a targeting moiety have great potential to achieve tissue and organ targeting. A key challenge in development of targeted liposomes is the capacity to attach and display the targeting entity on the particle. The ultimate goal of the project was to create a targeted-FAST peptide that would not disrupt the fusogenic properties of the p14 protein, but would target prostate cancer cells as well. For the first time, we present a detailed report on how to develop a p14 targeted protein to incorporate into liposomes. Evidence demonstrates that attachment of bombesin to the C-terminus of the p14 protein does not disrupt the functional capability and supports the findings found by Corcoran et al in the deletion studies of the C-terminus (Corcoran et al., 2004). However, unlike Corcoran et al who recognized that deletion of amino acids at the C-terminus decreased the rate of syncytium, we discovered that conjugation of bombesin to the C-terminus did not (Corcoran et al., 2004). P14-bombesin was able to create syncytia

in both functionality tests; vector transfection and protein assays. Furthermore, the attachment of bombesin did not change the properties of protein insertion and therefore the original OG detergent depletion method was used. Moreover, the SM2 Bio Beads used during dialysis did not inactivate the fusion moiety of p14 as Metsikko et al indicated in their study (Metsikko et al., 1986). Giving rise to the concept, that the C-terminus of p14 will tolerate the conjugation of a targeting peptide without destroying the fusogenic capability of the p14 FAST protein. Thus, p14 is a promising asset to targeted liposomal therapy, due to its tolerance of a targeting entity on the C-terminus.

We hypothesized that anti cancer therapeutics delivered in molecular targeted fusogenic liposomes will increase intracellular delivery and specificity for prostate cancer cells. Indeed, we found that the p14-bombesin liposomes did target PC3 cells specifically compared to non-cancerous BPH cells. In addition, bombesin conferred specific binding to the GRPR verified by receptor blocking analysis and silencing of the receptor. Although the methodology employed was not completely novel, the attachment of a targeting peptide to the p14 was a distinct feature. While fusogenic liposomes have provided an efficient tool for intracellular delivery, the incorporation of a targeting peptide allows for specific tissue and organ trafficking. In this study, we have engineered a functional navigating drug delivery system capable of targeting the GRPR expressing cells which is further strengthened by efficient intracellular delivery via the functional p14.

Delivery of DNA and siRNA has gained the attention of many researchers. The possibility to transport these nucleic acids would create a new generation of therapeutics. DNA vaccines have been used for decades, however if an adequate carrier could shield

the DNA from degradation *in vivo* the possibilities are endless. Wrapsomes have demonstrated a new class of liposomes possible to efficiently encapsulate the negatively charged amino acids. Herein, we describe preliminary evidence of the use of the platform in conjugation with the p14 peptide to further increase the efficacy of this delivery module. Wrapped Liposomes involves exploiting the cationic lipid nature to bind with the anionic DNA and wrapping this core within another lipid bilayer for fabrication of an unique wrapsome. We in turn capitalized on this distinctive encapsulation strategy and inserted our p14 protein to increase the efficacy of WS. We demonstrated that the key potential of WS was to not only entrap enough DNA to exert an effect on target cells but to decrease toxicity seen with traditional transfection reagents. Our very early studies indicate the potential of using the p14 protein to increase the delivery of nucleic acids. In this dissertation we provided evidence of delivery of DNA, however, the possibility of siRNA delivery is also capable. Therefore, the advent of this nanotechnology has provided key improvements to nucleic acid delivery in hopes of contributing to the therapy of human disease.

Limitations

Although this study has provided *in vitro* "proof of principle" evidence that p14-bombesin liposomes target PC3 cells, there are drawbacks associated with the lack of *in vivo* studies. Assessing the active targeting of the liposomes to the prostate cancer in an animal model would allow us to conclude that the p14-bombesin liposomes navigate specifically to prostate cancer specifically. The assessment of a therapeutic moiety is

needed to test the efficiency of the drug delivery platform. Finally, *in vivo* studies should be preformed to compare the tumour targeting and tumour growth inhibition.

4.2 Future Directions and Clinical Implications

Based on the above finding, the results of the current study contributed to a novel therapeutic platform for specific targeting of prostate cancer as well as successful intracellular delivery. These results have demonstrated that a targeting peptide can be conjugated to the C-terminus of the p14 protein and therefore creates endless opportunities to target other diseases organs and tissues. Using similar approaches baculovirus platforms could express a variety of targeting constructs. Other examples of targeting ligands to conjugate to p14 are Rb_p or RGD peptides. These peptides have been investigated to target tumour endothelial cells in angiogenic vessels within solid tumours by binding to integrins (Arap et al., 1998). Using these integrins we could target any type of tumour by directing the fusogenic liposomes to the endothelial of tumour vessels. Furthermore, with this therapeutic platform we could create liposomes that contained different targeting agents within one liposome population. Conjugating different targeting peptides, such a tumour targeting agent (bombesin) and an angiogenic integrin (RGD), liposomes would target both the tumour and the vasculature.

Non-invasive imaging would be greatly advantageous to monitor the targeted delivery of therapeutic agents as it would allow the real-time evaluation of biodistribution and tumour uptake. Furthermore, non-invasive modalities such as positron emission

tomography (PET) and single photon emission computed tomography (SPECT) would be useful to image the uptake of liposomes in prostate cancer. Creation of a dual non-invasive imaging and drug delivery system using liposomes labeled with radioisotopes such as ^{111}In. would allow the study of biodistribution of the prostate directed fusogenic liposomes using SPECT and/or PET imaging.

The administration of a gene of interest successfully results in expression of the therapeutic protein and thus the delivery of the large anionic DNA across the cell membrane is the most difficult endeavours. Wrapsomes have proved to deliver intact anionic nucleic acids and therefore this recombinant DNA technology has created opportunities for gene therapy for other diseases such as arteriosclerosis, cystic fibrosis, and other genetic disease. Using this unique lipid formulation that protects the nucleic acids from degradation in vivo also allows the opportunity to deliver siRNA.

Targeted technology encourages earlier deployment of therapeutics to treat prostate cancer which can increase the therapeutic index while decreasing side effects. There is an evident need for targeted therapy of prostate cancer to direct therapeutics to the site of cancer development. This research provides preliminary evidence of an effective alternative to current liposomal chemotherapy. This targeted fusogenic model would also be useful for the administration of other pharmacological agents and could also be used for non-invasive imaging. The targeted fusogenic liposomes engineered in this study has the potential to target disease sites while also penetrating the impermeable cell membrane, a “Swiss Army Knife” of liposomal carriers.

References

Ahne, W., Thomsen, I., & Winton, J. (1987). Isolation of a reovirus from the snake, python regius. brief report. *Archives of Virology, 94*(1-2), 135-139.

Allen, T. M., & Hansen, C. (1991). Pharmacokinetics of stealth versus conventional liposomes: Effect of dose. *Biochimica Et Biophysica Acta, 1068*(2), 133-141.

Allen, T. M., Mehra, T., Hansen, C., & Chin, Y. C. (1992). Stealth liposomes: An improved sustained release system for 1-beta-D-arabinofuranosylcytosine. *Cancer Research, 52*(9), 2431-2439.

Ananias, H. J., de Jong, I. J., Dierckx, R. A., van de Wiele, C., Helfrich, W., & Elsinga, P. H. (2008). Nuclear imaging of prostate cancer with gastrin-releasing-peptide-receptor targeted radiopharmaceuticals. *Current Pharmaceutical Design, 14*(28), 3033-3047.

Anastasi, A., Erspamer, V., & Bucci, M. (1971). Isolation and structure of bombesin and alytesin, 2 analogous active peptides from the skin of the european amphibians bombina and alytes. *Experientia, 27*(2), 166-167.

Andriole, G. L., Crawford, E. D., Grubb, R. L.,3rd, Buys, S. S., Chia, D., Church, T. R., et al. (2009). Mortality results from a randomized prostate-cancer screening trial. *The New England Journal of Medicine, 360*(13), 1310-1319.

Aprikian, A. G., Han, K., Chevalier, S., Bazinet, M., & Viallet, J. (1996). Bombesin specifically induces intracellular calcium mobilization via gastrin-releasing peptide receptors in human prostate cancer cells. *Journal of Molecular Endocrinology, 16*(3), 297-306.

Arap, W., Pasqualini, R., & Ruoslahti, E. (1998). Cancer treatment by targeted drug delivery to tumor vasculature in a mouse model. *Science (New York, N.Y.)*, *279*(5349), 377-380.

Bangham, A. D., & Horne, R. W. (1964). Negative staining of phospholipids and their structural modification by surface-active agents as observed in the electron microscope. *Journal of Molecular Biology*, *8*, 660-668.

Bangma, C. H. (2011). Active surveillance and radical prostatectomy. *European Journal of Cancer (Oxford, England : 1990)*, *47 Suppl 3*, S355-6.

Canadian Cancer Statistics. (2011). *National Cancer Institute of Canada.*

Casu, B. (1985). Structure and biological activity of heparin. *Advances in Carbohydrate Chemistry and Biochemistry*, *43*, 51-134.

Chernomordik, L. V., & Kozlov, M. M. (2003). Protein-lipid interplay in fusion and fission of biological membranes. *Annual Review of Biochemistry*, *72*, 175-207.

Cladera, J., Rigaud, J. L., Villaverde, J., & Dunach, M. (1997). Liposome solubilization and membrane protein reconstitution using chaps and chapso. *European Journal of Biochemistry / FEBS*, *243*(3), 798-804.

Coderch, L., Fonollosa, J., De Pera, M., Estelrich, J., De La Maza, A., & Parra, J. L. (2000). Influence of cholesterol on liposome fluidity by EPR. relationship with percutaneous absorption. *Journal of Controlled Release : Official Journal of the Controlled Release Society*, *68*(1), 85-95.

Corcoran, J. A., & Duncan, R. (2004). Reptilian reovirus utilizes a small type III protein with an external myristylated amino terminus to mediate cell-cell fusion. *Journal of Virology*, *78*(8), 4342-4351.

Corcoran, J. A., Syvitski, R., Top, D., Epand, R. M., Epand, R. F., Jakeman, D., et al. (2004). Myristoylation, a protruding loop, and structural plasticity are essential

features of a nonenveloped virus fusion peptide motif. *The Journal of Biological Chemistry, 279*(49), 51386-51394.

Demirgoz, D., Garg, A., & Kokkoli, E. (2008). PR_b-targeted PEGylated liposomes for prostate cancer therapy. *Langmuir : The ACS Journal of Surfaces and Colloids, 24*(23), 13518-13524.

Doherty, R., & Almallah, Z. (2011). Urinary incontinence after treatment for prostate cancer. *BMJ (Clinical Research Ed.), 343*, d6298.

Drulis-Kawa, Z., & Dorotkiewicz-Jach, A. (2010). Liposomes as delivery systems for antibiotics. *International Journal of Pharmaceutics, 387*(1-2), 187-198.

Duarte, S., Faneca, H., & de Lima, M. C. (2011). Non-covalent association of folate to lipoplexes: A promising strategy to improve gene delivery in the presence of serum. *Journal of Controlled Release : Official Journal of the Controlled Release Society, 149*(3), 264-272.

Duncan, R. (1996). The low pH-dependent entry of avian reovirus is accompanied by two specific cleavages of the major outer capsid protein mu 2C. *Virology, 219*(1), 179-189.

Duncan, R., Chen, Z., Walsh, S., & Wu, S. (1996). Avian reovirus-induced syncytium formation is independent of infectious progeny virus production and enhances the rate, but is not essential, for virus-induced cytopathology and virus egress. *Virology, 224*(2), 453-464.

Duncan, R., Corcoran, J., Shou, J., & Stoltz, D. (2004). Reptilian reovirus: A new fusogenic orthoreovirus species. *Virology, 319*(1), 131-140.

Duncan, R., Murphy, F. A., & Mirkovic, R. R. (1995). Characterization of a novel syncytium-inducing baboon reovirus. *Virology, 212*(2), 752-756.

Eidelman, O., Schlegel, R., Tralka, T. S., & Blumenthal, R. (1984). pH-dependent fusion induced by vesicular stomatitis virus glycoprotein reconstituted into phospholipid vesicles. *The Journal of Biological Chemistry, 259*(7), 4622-4628.

Ellison, L. F., Gibbons, L., & Canadian Cancer Survival Analysis Group. (2001). Five-year relative survival from prostate, breast, colorectal and lung cancer. *Health Reports / Statistics Canada, Canadian Centre for Health Information 13*(1), 23-34.

Farhood, H., Serbina, N., & Huang, L. (1995). The role of dioleoyl phosphatidylethanolamine in cationic liposome mediated gene transfer. *Biochimica Et Biophysica Acta, 1235*(2), 289-295.

Felgner, P. L., Gadek, T. R., Holm, M., Roman, R., Chan, H. W., Wenz, M., et al. (1987). Lipofection: A highly efficient, lipid-mediated DNA-transfection procedure. *Proceedings of the National Academy of Sciences of the United States of America, 84*(21), 7413-7417.

Gaberc-Porekar, V., & Menart, V. (2001). Perspectives of immobilized-metal affinity chromatography. *Journal of Biochemical and Biophysical Methods, 49*(1-3), 335-360.

Gabizon, A., Horowitz, A. T., Goren, D., Tzemach, D., Mandelbaum-Shavit, F., Qazen, M. M., et al. (1999). Targeting folate receptor with folate linked to extremities of poly(ethylene glycol)-grafted liposomes: In vitro studies. *Bioconjugate Chemistry*.

Gard, G., & Compans, R. W. (1970). Structure and cytopathic effects of nelson bay virus. *Journal of Virology, 6*(1), 100-106.

Gershon, H., Ghirlando, R., Guttman, S. B., & Minsky, A. (1993). Mode of formation and structural features of DNA-cationic liposome complexes used for transfection. *Biochemistry, 32*(28), 7143-7151.

Goldstein, A. S., Huang, J., Guo, C., Garraway, I. P., & Witte, O. N. (2010). Identification of a cell of origin for human prostate cancer. *Science (New York, N.Y.), 329*(5991), 568-571.

Gomella, L. G., Liu, X. S., Trabulsi, E. J., Kelly, W. K., Myers, R., Showalter, T., et al. (2011). Screening for prostate cancer: The current evidence and guidelines controversy. *The Canadian Journal of Urology*, *18*(5), 5875-5883.

Gorin, M. A., Eldefrawy, A., Ekwenna, O., & Soloway, M. S. (2011). Active surveillance for low-risk prostate cancer: Knowledge, acceptance and practice among urologists. *Prostate Cancer and Prostatic Diseases.*

Graversen, P. H., Nielsen, K. T., Gasser, T. C., Corle, D. K., & Madsen, P. O. (1990). Radical prostatectomy versus expectant primary treatment in stages I and II prostatic cancer. A fifteen-year follow-up. *Urology, 36*(6), 493-498.

Hansen, C. B., Kao, G. Y., Moase, E. H., Zalipsky, S., & Allen, T. M. (1995). Attachment of antibodies to sterically stabilized liposomes: Evaluation, comparison and optimization of coupling procedures. *Biochimica Et Biophysica Acta, 1239*(2), 133-144.

Ikegami, S., Yamakami, K., Ono, T., Sato, M., Suzuki, S., Yoshimura, I., et al. (2006). Targeting gene therapy for prostate cancer cells by liposomes complexed with anti-prostate-specific membrane antigen monoclonal antibody. *Human Gene Therapy, 17*(10), 997-1005.

Immordino, M. L., Dosio, F., & Cattel, L. (2006). Stealth liposomes: Review of the basic science, rationale, and clinical applications, existing and potential. *International Journal of Nanomedicine, 1*(3), 297-315.

Ito, M., Ikegami, M., Shiroki, K., & Tagaya, I. (1964). Studies on the multiplication of simian virus 40 (vascuolating virus) by means of fluorescent antibody technique. *Japanese Journal of Medical Science & Biology*, *17*, 179-193.

Jacobsen, S. J., Katusic, S. K., Bergstralh, E. J., Oesterling, J. E., Ohrt, D., Klee, G. G., et al. (1995). Incidence of prostate cancer diagnosis in the eras before and after serum prostate-specific antigen testing. *JAMA : The Journal of the American Medical Association, 274*(18), 1445-1449.

Jayanna, P. K., Torchilin, V. P., & Petrenko, V. A. (2009). Liposomes targeted by fusion phage proteins. *Nanomedicine, 5*(1), 83-89.

Karakiewicz, P. I., & Aprikian, A. G. (1998). Prostate cancer: 5. diagnostic tools for early detection. *CMAJ, 159*(9), 1139-1146.

Kasperzyk, J. L., Shappley, W. V.,3rd, Kenfield, S. A., Mucci, L. A., Kurth, T., Ma, J., et al. (2011). Watchful waiting and quality of life among prostate cancer survivors in the physicians' health study. *The Journal of Urology, 186*(5), 1862-1867.

Kaye, S. B., & Richardson, V. J. (1979). Potential of liposomes as drug-carriers in cancer chemotherapy: A review. *Cancer Chemotherapy and Pharmacology, 3*(2), 81-85.

Kobayashi, S., Nakase, I., Kawabata, N., Yu, H. H., Pujals, S., Imanishi, M., et al. (2009). Cytosolic targeting of macromolecules using a pH-dependent fusogenic peptide in combination with cationic liposomes. *Bioconjugate Chemistry, 20*(5), 953-959.

Kuijpers, S. A., Coimbra, M. J., Storm, G., & Schiffelers, R. M. (2010). Liposomes targeting tumour stromal cells. *Molecular Membrane Biology, 27*(7), 328-340.

Lawson, D. A., Zong, Y., Memarzadeh, S., Xin, L., Huang, J., & Witte, O. N. (2010). Basal epithelial stem cells are efficient targets for prostate cancer initiation. *PNAS, 107*(6), 2610-2615.

Lee, C. M., Jeong, H. J., Cheong, S. J., Kim, E. M., Kim, D. W., Lim, S. T., et al. (2010). Prostate cancer-targeted imaging using magnetofluorescent polymeric nanoparticles functionalized with bombesin. *Pharmaceutical Research, 27*(4), 712-721.

Leser, G. P., Ector, K. J., & Lamb, R. A. (1996). The paramyxovirus simian virus 5 hemagglutinin-neuraminidase glycoprotein, but not the fusion glycoprotein, is internalized via coated pits and enters the endocytic pathway. *Molecular Biology of the Cell, 7*(1), 155-172.

Ley, C., Holtmann, D., Mangold, K. M., & Schrader, J. (2011). Immobilization of histidine-tagged proteins on electrodes. *Colloids and Surfaces.B, Biointerfaces, 88*(2), 539-551.

Liautard, J., Philippot, J. R., & Liautard, J. P. (1991). Encapsulation of drugs into large unilamellar liposomes prepared by an extemporaneous method. *Journal of Microencapsulation, 8*(3), 381-389.

Lichtenberg, D., Robson, R. J., & Dennis, E. A. (1983). Solubilization of phospholipids by detergents. structural and kinetic aspects. *Biochimica Et Biophysica Acta, 737*(2), 285-304.

Liu, D., Mori, A., & Huang, L. (1992). Role of liposome size and RES blockade in controlling biodistribution and tumor uptake of GM1-containing liposomes. *Biochimica Et Biophysica Acta, 1104*(1), 95-101.

Lutsiak, M. E., Kwon, G. S., & Samuel, J. (2002). Analysis of peptide and lipopeptide content in liposomes. *Journal of Pharmacy & Pharmaceutical Science, 5*(3), 279-284.

Mader, J. S., Richardson, A., Salsman, J., Top, D., de Antueno, R., Duncan, R., et al. (2007). Bovine lactoferricin causes apoptosis in jurkat T-leukemia cells by sequential permeabilization of the cell membrane and targeting of mitochondria. *Experimental Cell Research, 313*(12), 2634-2650.

Maeda, H., Wu, J., Sawa, T., Matsumura, Y., & Hori, K. (2000). Tumor vascular permeability and the EPR effect in macromolecular therapeutics: A review. *Journal of Controlled Release, 65*(1-2), 271-284.

Maruyama, K. (2002). PEG-immunoliposome. *Bioscience Reports, 22*(2), 251-266.

Maruyama, K. (2011). Intracellular targeting delivery of liposomal drugs to solid tumors based on EPR effects. *Advanced Drug Delivery Reviews, 63*(3), 161-169.

Matsumura, Y., & Maeda, H. (1986). A new concept for macromolecular therapeutics in cancer chemotherapy: Mechanism of tumoritropic accumulation of proteins and the antitumor agent smancs. *Cancer Research, 46*(12 Pt 1), 6387-6392.

Mayer, L. D., Tai, L. C., Ko, D. S., Masin, D., Ginsberg, R. S., Cullis, P. R., et al. (1989). Influence of vesicle size, lipid composition, and drug-to-lipid ratio on the biological activity of liposomal doxorubicin in mice. *Cancer Research, 49*(21), 5922-5930.

Metsikko, K., van Meer, G., & Simons, K. (1986). Reconstitution of the fusogenic activity of vesicular stomatitis virus. *The EMBO Journal, 5*(13), 3429-3435.

Meulendyke, K. A., Wurth, M. A., McCann, R. O., & Dutch, R. E. (2005). Endocytosis plays a critical role in proteolytic processing of the hendra virus fusion protein. *Journal of Virology, 79*(20), 12643-12649.

Mishra, S., Webster, P., & Davis, M. E. (2004). PEGylation significantly affects cellular uptake and intracellular trafficking of non-viral gene delivery particles. *European Journal of Cell Biology, 83*(3), 97-111.

Moret, I., Esteban Peris, J., Guillem, V. M., Benet, M., Revert, F., Dasi, F., et al. (2001). Stability of PEI-DNA and DOTAP-DNA complexes: Effect of alkaline pH, heparin and serum. *Journal of Controlled Release : Official Journal of the Controlled Release Society, 76*(1-2), 169-181.

Nobs, L., Buchegger, F., Gurny, R., & Allemann, E. (2004). Current methods for attaching targeting ligands to liposomes and nanoparticles. *Journal of Pharmaceutical Sciences, 93*(8), 1980-1992.

Park, J. W. (2002). Liposome-based drug delivery in breast cancer treatment. *Breast Cancer Research : BCR, 4*(3), 95-99.

Paternostre, M. T., Roux, M., & Rigaud, J. L. (1988). Mechanisms of membrane protein insertion into liposomes during reconstitution procedures involving the use of detergents. 1. solubilization of large unilamellar liposomes (prepared by reverse-

phase evaporation) by triton X-100, octyl glucoside, and sodium cholate. *Biochemistry, 27*(8), 2668-2677.

Peisajovich, S. G., Epand, R. F., Epand, R. M., & Shai, Y. (2002). Sendai virus N-terminal fusion peptide consists of two similar repeats, both of which contribute to membrane fusion. *European Journal of Biochemistry / FEBS, 269*(17), 4342-4350.

Petri, W. A.,Jr, & Wagner, R. R. (1979). Reconstitution into liposomes of the glycoprotein of vesicular stomatitis virus by detergent dialysis. *The Journal of Biological Chemistry, 254*(11), 4313-4316.

Remaut, K., Lucas, B., Braeckmans, K., Demeester, J., & De Smedt, S. C. (2007). Pegylation of liposomes favours the endosomal degradation of the delivered phosphodiester oligonucleotides. *Journal of Controlled Release, 117*(2), 256-266.

Reubi, J. C., Wenger, S., Schmuckli-Maurer, J., Schaer, J. C., & Gugger, M. (2002). Bombesin receptor subtypes in human cancers: Detection with the universal radioligand (125)I-[D-TYR(6), beta-ALA(11), PHE(13), NLE(14)] bombesin(6-14). *Clinical Cancer Research : An Official Journal of the American Association for Cancer Research, 8*(4), 1139-1146.

Rigaud, J. L., Paternostre, M. T., & Bluzat, A. (1988). Mechanisms of membrane protein insertion into liposomes during reconstitution procedures involving the use of detergents. 2. incorporation of the light-driven proton pump bacteriorhodopsin. *Biochemistry, 27*(8), 2677-2688.

Safavy, A., Khazaeli, M. B., Qin, H., & Buchsbaum, D. J. (1997). Synthesis of bombesin analogues for radiolabeling with rhenium-188. *Cancer, 80*(12 Suppl), 2354-2359.

Sakurai, Y., Hatakeyama, H., Sato, Y., Akita, H., Takayama, K., Kobayashi, S., et al. (2011). Endosomal escape and the knockdown efficiency of liposomal-siRNA by the fusogenic peptide shGALA. *Biomaterials, 32*(24), 5733-5742.

Schwendener, R. A., & Schott, H. (2010). Liposome formulations of hydrophobic drugs. *Methods in Molecular Biology (Clifton, N.J.), 605*, 129-138.

Shmulevitz, M., & Duncan, R. (2000). A new class of fusion-associated small transmembrane (FAST) proteins encoded by the non-enveloped fusogenic reoviruses. *The EMBO Journal, 19*(5), 902-912.

Shmulevitz, M., Epand, R. F., Epand, R. M., & Duncan, R. (2004). Structural and functional properties of an unusual internal fusion peptide in a nonenveloped virus membrane fusion protein. *Journal of Virology*, *78*(6), 2808-2818.

Shmulevitz, M., Salsman, J., & Duncan, R. (2003). Palmitoylation, membrane-proximal basic residues, and transmembrane glycine residues in the reovirus p10 protein are essential for syncytium formation. *Journal of Virology*, *77*(18), 9769-9779.

Shmulevitz, M., Yameen, Z., Dawe, S., Shou, J., O'Hara, D., Holmes, I., et al. (2002). Sequential partially overlapping gene arrangement in the tricistronic S1 genome segments of avian reovirus and nelson bay reovirus: Implications for translation initiation. *Journal of Virology, 76*(2), 609-618.

Siegel, T., Moul, J. W., Spevak, M., Alvord, W. G., & Costabile, R. A. (2001). The development of erectile dysfunction in men treated for prostate cancer. *The Journal of Urology, 165*(2), 430-435.

Singh, M. (1999). Transferrin as A targeting ligand for liposomes and anticancer drugs. *Current Pharmaceutical Design, 5*(6), 443-451.

Sofou, S. (2007). Surface-active liposomes for targeted cancer therapy. *Nanomedicine (London, England), 2*(5), 711-724.

Steinmetz, N. F., Ablack, A. L., Hickey, J. L., Ablack, J., Manocha, B., Mymryk, J. S., et al. (2011a). Intravital imaging of human prostate cancer using viral nanoparticles targeted to gastrin-releasing peptide receptors. *Small, 7*(12), 1664-1672.

Struck, D. K., Hoekstra, D., & Pagano, R. E. (1981). Use of resonance energy transfer to monitor membrane fusion. *Biochemistry, 20*(14), 4093-4099.

Top, D., de Antueno, R., Salsman, J., Corcoran, J., Mader, J., Hoskin, D., et al. (2005). Liposome reconstitution of a minimal protein-mediated membrane fusion machine. *The EMBO Journal, 24*(17), 2980-2988.

Top, D., Read, J. A., Dawe, S. J., Syvitski, R. T., & Duncan, R. (2011). Cell-cell membrane fusion induced by the p15 fusion-associated small transmembrane (FAST) protein requires a novel fusion peptide motif containing a myristoylated polyproline type II helix. *The Journal of Biological Chemistry,*

Tran, A., Berard, A., & Coombs, K. M. (2009). Growth and maintenance of quail fibrosarcoma QM5 cells. *Current Protocols in Microbiology, Appendix 4,* Appendix 4G.

Tsai, J. T., Furstoss, K. J., Michnick, T., Sloane, D. L., & Paul, R. W. (2002). Quantitative physical characterization of lipid-polycation-DNA lipopolyplexes. *Biotechnology and Applied Biochemistry, 36*(Pt 1), 13-20.

Uziely, B., Jeffers, S., Isacson, R., Kutsch, K., Wei-Tsao, D., Yehoshua, Z., et al. (1995). Liposomal doxorubicin: Antitumor activity and unique toxicities during two complementary phase I studies. *Journal of Clinical Oncology : Official Journal of the American Society of Clinical Oncology, 13*(7), 1777-1785.

Varvarigou, A., Bouziotis, P., Zikos, C., Scopinaro, F., & De Vincentis, G. (2004). Gastrin-releasing peptide (GRP) analogues for cancer imaging. *Cancer Biotherapy & Radiopharmaceuticals, 19*(2), 219-229.

Wang, T., Yang, S., Petrenko, V. A., & Torchilin, V. P. (2010). Cytoplasmic delivery of liposomes into MCF-7 breast cancer cells mediated by cell-specific phage fusion coat protein. *Molecular Pharmaceutics, 7*(4), 1149-1158.

Xu, Y., & Szoka, F. C.,Jr. (1996). Mechanism of DNA release from cationic liposome/DNA complexes used in cell transfection. *Biochemistry, 35*(18), 5616-5623.

Yagi, N., Manabe, I., Tottori, T., Ishihara, A., Ogata, F., Kim, J. H., et al. (2009). A nanoparticle system specifically designed to deliver short interfering RNA inhibits tumor growth in vivo. *Cancer Research, 69*(16), 6531-6538.

Yamauchi, M., Kusano, H., Saito, E., Iwata, T., Nakakura, M., Kato, Y., et al. (2006). Development of wrapped liposomes: Novel liposomes comprised of polyanion drug and cationic lipid complexes wrapped with neutral lipids. *Biochimica Et Biophysica Acta, 1758*(1), 90-97.

Yamauchi, M., Kusano, H., Saito, E., Iwata, T., Nakakura, M., Kato, Y., et al. (2006). Improved formulations of antisense oligodeoxynucleotides using wrapped liposomes. *Journal of Controlled Release, 114*(2), 268-275.

Yu, B., Tai, H. C., Xue, W., Lee, L. J., & Lee, R. J. (2010). Receptor-targeted nanocarriers for therapeutic delivery to cancer. *Molecular Membrane Biology, 27*(7), 286-298.

Yu, W., Pirollo, K. F., Rait, A., Yu, B., Xiang, L. M., Huang, W. Q., et al. (2004). A sterically stabilized immunolipoplex for systemic administration of a therapeutic gene. *Gene Therapy, 11*(19), 1434-1440.

Zelphati, O., & Szoka, F. C.,Jr. (1996). Mechanism of oligonucleotide release from cationic liposomes. *Proceedings of the National Academy of Sciences of the United States of America, 93*(21), 11493-11498.

Zhou, X., & Huang, L. (1994). DNA transfection mediated by cationic liposomes containing lipopolylysine: Characterization and mechanism of action. *Biochimica Et Biophysica Acta, 1189*(2), 195-203.

Zuhorn, I. S., Bakowsky, U., Polushkin, E., Visser, W. H., Stuart, M. C., Engberts, J. B., et al. (2005). Nonbilayer phase of lipoplex-membrane mixture determines endosomal escape of genetic cargo and transfection efficiency. *Molecular Therapy: The Journal of the American Society of Gene Therapy, 11*(5), 801-810.

.

Appendix

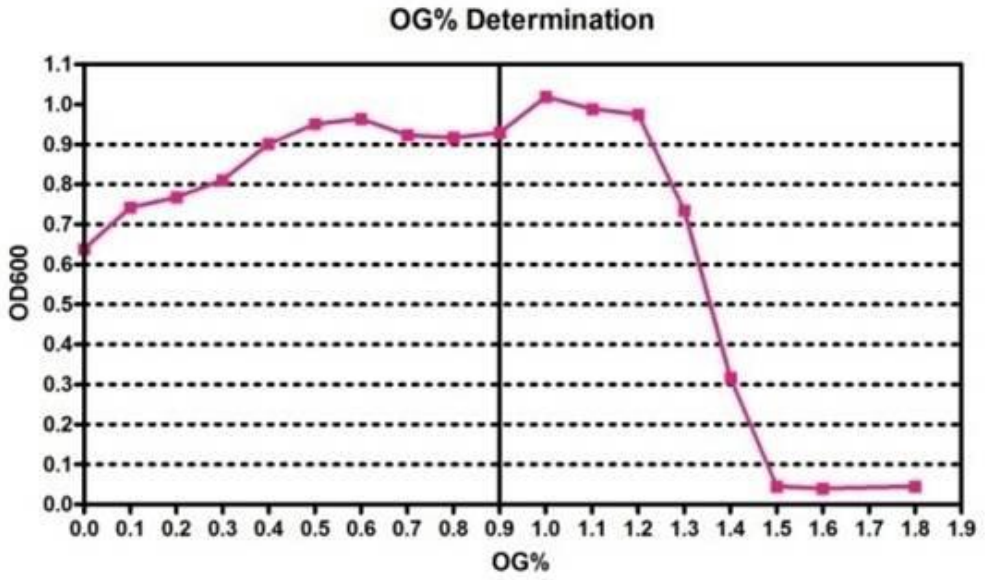

Appendix A Analysis of the % OG need to insert the p14 protein
Differing concentrations of n-Octyl b-D-glucopyranoside (OG) was added to liposomes and the optical density (OD600) was measured. This assay determines the necessary amount of OG to change the fluidity of the lipid membrane without solubilizing the liposomes.

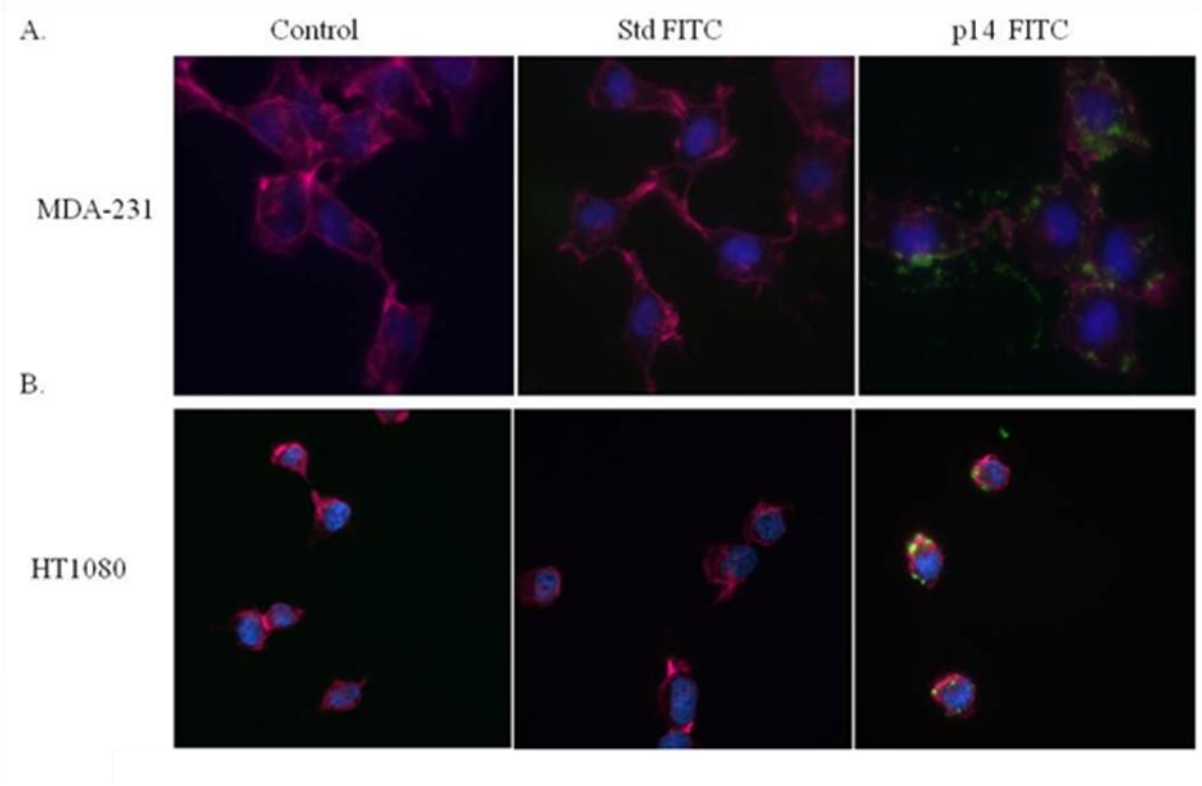

Appendix B p14-Liposomes increase intracellular FITC delivery

Liposome uptake analysis of FITC, delivered by standard (Std) liposomes (no protein) and fusogenic liposomes (p14 protein). Representative fluorescent images of one field of view of A) MDA-MB-231 and B) HT1080 cells at 20 X magnification. The cells were stained with a nuclear stain (DAPI, blue) and an actin filament stain (phalloidin). The green fluorescent signal represents the intracellular FITC uptake.

Appendix C Confirmation of the p14-Bombesin Sequence.

P14-bombesin sequence was confirmed by DNA analysis at Robarts Research Institute. The sequence in black corresponds to the original sequence generated by Vector NTI ® Software (Invitrogen) including the enterokinase site (purple highlight), histidine tag (green highlight), bombesin (yellow highlight) and the stop codon (TAA). The sequence in purple represents the forward sequencing and the green base pairs represents the reverse sequence returned from the Robarts. Verifying bombesin was successfully cloned to the C-terminus of p14.

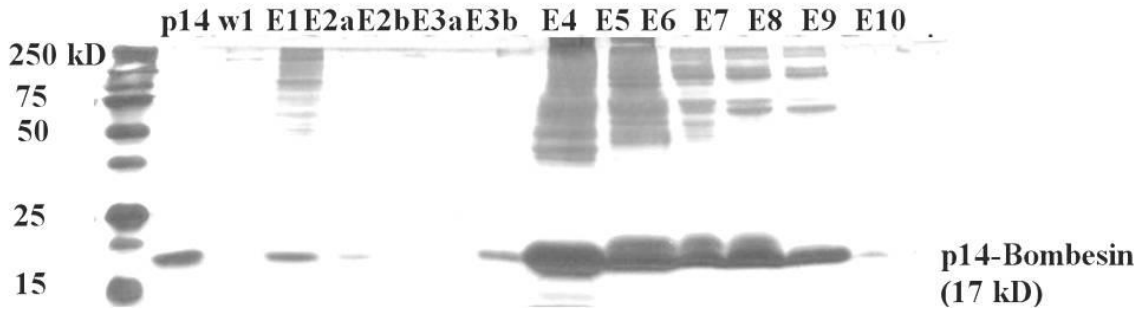

Appendix D Silver Stain analysis of the different fractions eluted from the ion exchange column from varying the ionic strength and pH of the buffers.
Aliquots 7 ug of protein (per elution) were analyzed using SDS-PAGE and protein bands were visualized by silver staining. Native p14 was used as a standard (p14 std) to indicate the relative migration. Lanes E4 – E8 show typical elution profile of purified p14-bombesin.

Mole Ratio		1ug
	DOTAP	DNA
mol	0.0000005	2.6656E-10
DOTAP:DNA Charge ratio	1	0.000533 12

	DOTAP	DNA
mole	0.0000005	2.63539E-12
Number of molecules	3.011E+17	1.58703E+12
Number pos charges	3.011E+17	7.30036E+13
ratio of pos:neg charges	4124.4565	1

Appendix E Calculation to determine the concentration of DOTAP to the amount of DNA present to result in a 1:1 ratio

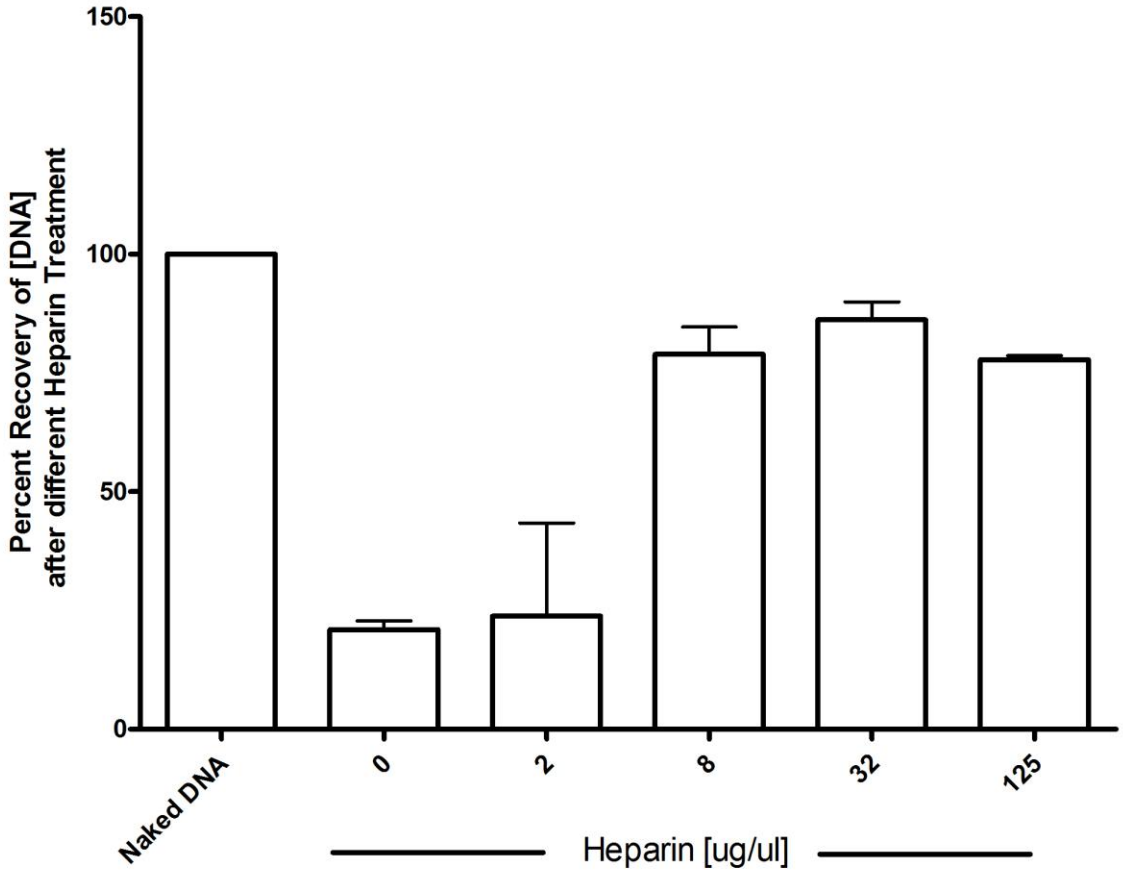

Appendix F Determination of heparin concentration to displace DNA from the DOTAP using PicoGreen fluorescent analysis

Increasing the concentration of heparin to 125 μg/μl did not increase the amount of DNA released from the DOTAP core compared to 8μg/μl. Any concentration from 8-125 μg/μl will sufficiently displace DOTAP exposing DNA to bind to fluorescent probes for quantification.

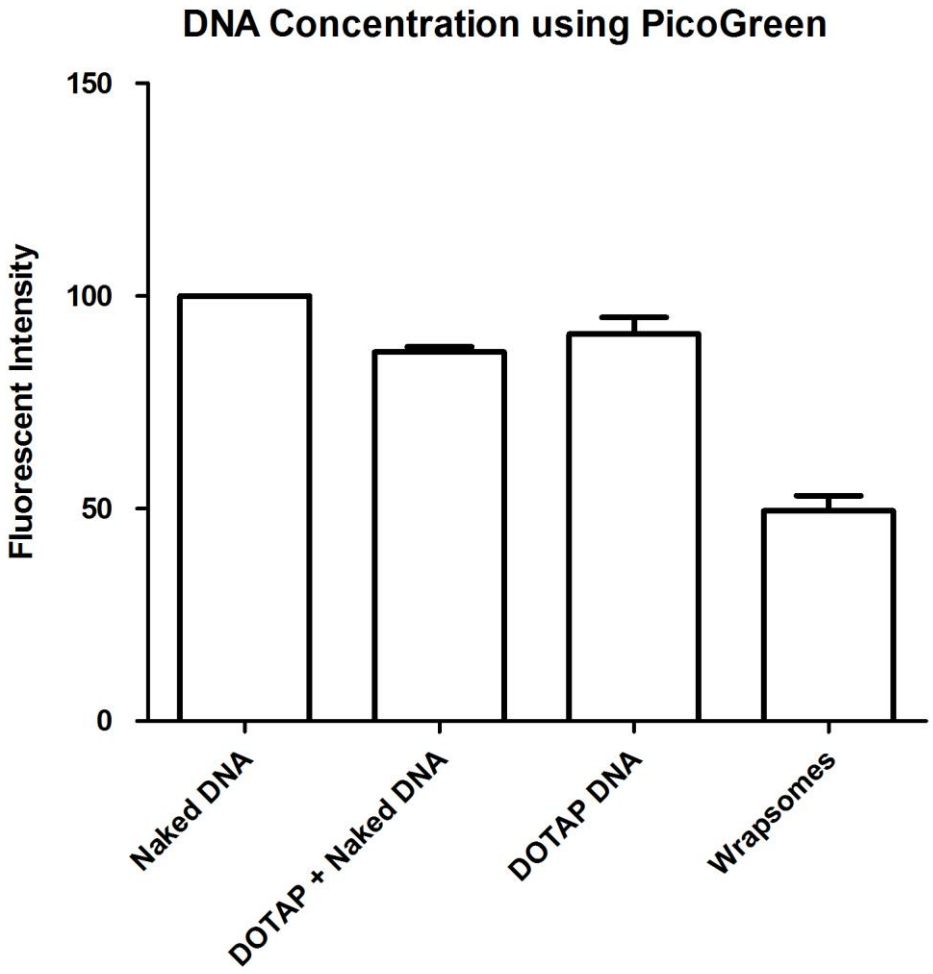

Appendix G Calculating DNA encapsulation efficiency in WS

Picogreen DNA analysis using heparin to displace DOTAP from the DNA, WS had ~50% encapsulation efficiency. This assay is not qualitative as the displacement of DOTAP is not definite and thus remains to interfere with the assay.

Curriculum Vitae

Rae-Lynn Nesbitt

Education

MSc. Medical Biophysics Candidate *(2009- Present)*
University of Western Ontario, London, ON, Canada

B.Sc. Hon Biology *(2003-2009)*
University of Western Ontario, London, ON, Canada

Academic Honours/ Scholarships

2010 Schulich Entrance Award, University of Western Ontario, London, ON, Canada, $6900

2010 Translational Breast Cancer Studentship, London Regional Cancer Program, London, ON, Canada, $12,850

2010 CIHR Strategic Training Program in Cancer Research and Technology Transfer (CaRTT STP), London Regional Cancer Program, London, ON, Canada $12,850

2010 Lawson Research Day Poster Award, London, ON, Canada, $200

2009 Schulich Entrance Award, University of Western Ontario, London, ON, Canada, $6900

2003 Entrance Award Scholarship, University of Western Ontario, London, ON, Canada, $2000

Research/ Laboratory Experience

Summer 2009 **Summer Research Project**
London Regional Cancer Centre and University Hospital, London, ON.
Title: Inhibiting ischemia reperfusion injury in rat kidney's by silencing ICAM-1 and E-selectin with siRNA
Supervisor: Dr. Gabriel Chan and Dr. John Lewis

Jan.-April 2009 **Honour's Research Thesis Project**
Department of Biology, University of Western Ontario, London, ON.

Title: The *in vitro* suppression of ICAM-1 and E-selectin in LPS-stimulated human umbilical vein endothelial cells
Supervisor: Dr. Gabriel Chan

Teaching Experience

2011-Present **Undergraduate Teaching Assistant**
University of Western Ontario, London, ON, Canada

- Anatomy and Cell Biology, Translational Cancer Research Class
- Prepared seminar material for melanoma debates
- Responsible for assessing performance

Publications

Articles:

1. Lu, C., McFarland, M.S., **Nesbitt, R.**, Williams, A.K., Chan, S., Gomez-Lemus, J., Autran, A.M., Al-Zahrani, A., Chin, J., Izawa, J., Luyt, L.G., Lewis, J.D. (2011) Ghrelin Receptor as a Novel Imaging Target for Prostatic Neoplasms. *The Prostate*.

Manuscripts:

1. Pink, D., Manocha, B., **Nesbitt, R**., Duncan, R., Zijlstra, A., Lewis, J. (2011) Active intracellular delivery using fusogenic liposomes significantly improves the efficacy of liposomal docetaxel. (In preparation)

Patents:

1. US Provisional Patent, “Molecular targeted fusogenic liposomes”, (Inventors: Lewis, J.D., **Nesbitt, R.**, Duncan, R., de Antueno, R.)

Abstracts (Published):

1. **Nesbitt, R**., Pink, D., Duncan, R., Zijlstra, A., Lewis, J. (2011) Targeted Non-Invasive Therapy of Prostate Cancer using Fusogenix Liposomes. *American Association for Cancer Research Conference Meeting Abstracts*. Apr 2008: 3224.

Presentations:

1. **Nesbitt, R**., Pink, D., Duncan, R., Lewis, J. (2011) Targeted Therapy of Prostate Cancer using Fusogenic Liposomes. *Nano Drug Delivery Symposium.* University of Utah, Salt Lake City, Utah.

2. **Nesbitt, R**., Pink, D., Duncan, R., Lewis, J. (2011) Targeted Therapy of Prostate Cancer using Fusogenic Liposomes. *CaRTT Oncology Research & Education Day,* Lamplighter Inn, London, ON.

3. **Nesbitt, R**., Pink, D., Duncan, R., Zijlstra, A., Lewis, J. (2011) Targeted Non-Invasive Therapy of Prostate Cancer using Fusogenix Liposomes. *2011 AACR Annual Meeting*, Orange County Convention Centre, Orlando, FL.

4. Pink, D. **Nesbitt, R**., Silver, T., Duncan, R., Zijlstra, A., Lewis, J. (2010) The efficacy of liposomal Docetaxel is significantly improved by Fusogenix. *International Liposome Research Days*, University of British Columbia, Vancouver, BC.

5. **Nesbitt, R**., Pink, D., Duncan, R., Lewis, J. (2010) Targeted Non-Invasive Imaging and Therapy of Prostate Cancer using Fusogenic Liposomes. *Lawson Health Research Institute - Research Day*, London Convention Centre, London, ON. ***Poster Award***

6. **Nesbitt, R**., Pink, D., Duncan, R., Lewis, J. (2010) Targeted Non-Invasive Imaging and Therapy of Prostate Cancer using Fusogenic Liposomes. *CaRTT Oncology Research & Education Day,* Lamplighter Inn, London, ON.

7. **Nesbitt, R**., Ablack, A., Ablack, J., Hayden, D., Lewis, J., Hill, K., Chan, G. (2009). The *in vitro* suppression of ICAM-1 and E-selectin in LPS-stimulated human umbilical vein endothelial cells. *Honours Biology Thesis Presentation*, University of Western Ontario, London, ON.